

Natural multi-Higgs model with dark matter and CP violation

B. Grzadkowski*

Institute of Theoretical Physics, University of Warsaw, Hoża 69, PL-00-681 Warsaw, Poland

O. M. Ogreid†

Bergen University College, Bergen, Norway

P. Osland‡

Department of Physics and Technology, University of Bergen, Postboks 7803, N-5020 Bergen, Norway

(Received 20 April 2009; published 9 September 2009)

We explore an extension of the inert doublet model which allows also for CP violation in the Higgs sector. This necessitates two noninert doublets. The lightest neutral scalar of the inert doublet is a candidate for dark matter. Scanning over parameters we preserve the abundance of the dark matter in agreement with the WMAP data. We also impose all relevant collider and theoretical constraints to determine the allowed parameter space for which both the dark matter is appropriate and CP is violated. In addition we find regions where the cutoff of the model originating from naturality arguments can be substantially lifted compared to its standard model value, reaching $\sim 2\text{--}3$ TeV.

DOI: [10.1103/PhysRevD.80.055013](https://doi.org/10.1103/PhysRevD.80.055013)

PACS numbers: 12.60.Fr, 14.80.Cp, 95.30.Cq

I. INTRODUCTION

It is widely believed that the standard model (SM) of electroweak interactions is only an effective low-energy theory valid below a certain energy scale Λ , which is supposed to be of the order of 1 TeV. This view is based on the fact that radiative corrections, δm_h^2 , to the Higgs boson mass squared (m_h^2) tend to increase the mass up to Λ , implying a necessary fine-tuning. This is the celebrated little hierarchy problem or the “LEP paradox” [1]. In order to retain a meaningful perturbative expansion above ~ 1 TeV, a high level of fine-tuning between m_h and Λ is necessary to suppress δm_h^2 relative to m_h^2 ; see e.g. [2]. Other well-known problems of the SM are the lack of a candidate for the dark matter (DM) and too little CP violation that could make the electroweak baryogenesis viable [3]. In that context the SM scalar sector has to be modified as the phase transition within a single Higgs doublet is too slow for baryogenesis [3].

Our goal here is to outline a model that ameliorates the little hierarchy problem (lifting Λ at least to ~ 2 TeV) while providing extra sources of CP violation needed for baryogenesis as well as a realistic abundance of dark matter. We will focus on extending the Higgs sector of the SM by adding extra Higgs doublets since that could also help to make the electroweak phase transition fast enough; see [4].

In general there are two possibilities to alleviate the little hierarchy problem: (i) suppression of the radiative corrections, and/or (ii) an increase of the Higgs mass. Well-known examples of the first strategy are supersymmetric

extensions of the SM, however in fact that could be achieved to some extent even through very modest means, e.g. by introducing just one extra real scalar singlet to the SM [5] (although some fine-tuning is necessary). The second possibility has recently been followed by Barbieri, Hall, and Rychkov [6].¹ The idea is to introduce an extra scalar doublet η (the inert doublet) which does not couple to the SM fermions as a consequence of a Z_2 symmetry: $\eta \rightarrow -\eta$ (all other fields are neutral under the symmetry). Since it is required that $\langle \eta \rangle = 0$, the symmetry remains unbroken, therefore it can provide a DM candidate. Since the inert doublet contributes to gauge-boson two-point Green’s functions the SM-like Higgs boson could be as heavy as 400–600 GeV, ameliorating the little hierarchy problem this way. Also the DM constraints could be satisfied choosing masses of the scalar and pseudoscalar components of the inert Higgs of the order of 80 GeV. The analysis of [9] reveals also another solution for the DM candidate, such that scalar and pseudoscalar masses are much heavier, ≥ 500 GeV. The model in very simple terms avoids the little hierarchy problem for the lighter (inert) scalars as they just do not couple to fermions, so, in particular, not to the top quark. The only drawback is that the model is so restricted by the Z_2 symmetry that it does not allow for CP violation in the Higgs potential; this is the issue that we would like to address here. There are two simple extensions of the inert doublet model (IDM) that can accommodate CP violation:

- (i) Combining the standard 2-Higgs-doublet model (2HDM) with an inert scalar doublet η (in other

* Bohdan.Grzadkowski@fuw.edu.pl

† omo@hib.no

‡ per.osland@ift.uib.no

¹The model was proposed earlier in [7] as a possible solution to the DM problem, and its collider phenomenology was then discussed in [8].

words replacing the SM Higgs doublet of the IDM by *two* doublets).

(ii) Adding a complex singlet scalar to the IDM.

This paper is devoted to the first of these extensions. It is worth emphasizing that this scenario is not just a simple sum of the 2HDM and the IDM. Although some theoretical and experimental constraints which are applicable here are (to leading order) identical to those of the 2HDM (just because the inert doublet does not couple to fermions), there are also important exceptions. These concern the oblique parameters T and S , the amount of DM, and the issue of positivity of the scalar potential (vacuum stability):

- (i) The extra inert degrees of freedom transform as an $SU(2)$ doublet, so they couple to the vector bosons and therefore contribute to the oblique parameters, modifying the standard 2HDM predictions.
- (ii) The neutral components of the inert doublet are candidates for DM, and since the inert doublet couples to the 2HDM doublets, the amplitudes for DM annihilation are in general influenced in a nontrivial way by the extension of the noninert sector.
- (iii) Even under simplifying assumptions, the scalar potential for the 2HDM extended by the inert doublet has a rich structure, so that the condition for positivity is much more involved than a simple superposition of conditions needed for the 2HDM and the IDM separately.

The paper is organized as follows. In Sec. II we introduce the model and define some notation. In Sec. III we define some benchmarks for the inert sector, and in Sec. IV we present the strategy adopted to search for allowed regions in the parameter space of the model. Sections V and VI are devoted to reviews of theoretical and experimental constraints. In Sec. VII we show some regions of parameters of the model that are compatible with all the constraints, and in Sec. VIII we summarize.

Technical details on positivity, CP conservation, and necessary basis transformations are collected in Appendixes A, B, and C.

II. INERT-PLUS-TWO-DOUBLET MODEL: IDM2

A. The potential

Introduction of two doublets, $\Phi_{1,2}$ leads in general to flavor-changing neutral currents in Yukawa couplings. To avoid those one can impose an extra Z'_2 symmetry such that $\Phi_1 \rightarrow -\Phi_1$ and $u_R \rightarrow -u_R$ (all other fields are neutral). The model then has $Z_2 \times Z'_2$, where the first factor is the inert doublet Z_2 : $\eta \rightarrow -\eta$ (all other fields are neutral). The potential reads

$$V(\Phi_1, \Phi_2, \eta) = V_{12}(\Phi_1, \Phi_2) + V_3(\eta) + V_{123}(\Phi_1, \Phi_2, \eta), \quad (2.1)$$

where

$$\begin{aligned} V_{12}(\Phi_1, \Phi_2) = & -\frac{1}{2}\{m_{11}^2\Phi_1^\dagger\Phi_1 + m_{22}^2\Phi_2^\dagger\Phi_2 \\ & + [m_{12}^2\Phi_1^\dagger\Phi_2 + \text{H.c.}]\} + \frac{\lambda_1}{2}(\Phi_1^\dagger\Phi_1)^2 \\ & + \frac{\lambda_2}{2}(\Phi_2^\dagger\Phi_2)^2 + \lambda_3(\Phi_1^\dagger\Phi_1)(\Phi_2^\dagger\Phi_2) \\ & + \lambda_4(\Phi_1^\dagger\Phi_2)(\Phi_2^\dagger\Phi_1) \\ & + \frac{1}{2}[\lambda_5(\Phi_1^\dagger\Phi_2)^2 + \text{H.c.}], \end{aligned} \quad (2.2)$$

$$V_3(\eta) = m_\eta^2\eta^\dagger\eta + \frac{\lambda_\eta}{2}(\eta^\dagger\eta)^2, \quad (2.3)$$

$$\begin{aligned} V_{123}(\Phi_1, \Phi_2, \eta) = & \lambda_{1133}(\Phi_1^\dagger\Phi_1)(\eta^\dagger\eta) + \lambda_{2233}(\Phi_2^\dagger\Phi_2) \\ & \times (\eta^\dagger\eta) + \lambda_{1331}(\Phi_1^\dagger\eta)(\eta^\dagger\Phi_1) \\ & + \lambda_{2332}(\Phi_2^\dagger\eta)(\eta^\dagger\Phi_2) \\ & + \frac{1}{2}[\lambda_{1313}(\Phi_1^\dagger\eta)^2 + \text{H.c.}] \\ & + \frac{1}{2}[\lambda_{2323}(\Phi_2^\dagger\eta)^2 + \text{H.c.}] \end{aligned} \quad (2.4)$$

Here, λ_{1133} , λ_{2233} , λ_{1331} , and λ_{2332} are real, whereas λ_{1313} and λ_{2323} can be complex. Disregarding Φ_2 , the correspondence with the notation of [6] would be

$$(m_\eta, \lambda_\eta, \lambda_{1133}, \lambda_{1331}, \lambda_{1313}) \leftrightarrow (\mu_2, 2\lambda_2, \lambda_3, \lambda_4, \lambda_5). \quad (2.5)$$

In $V_1(\Phi_1, \Phi_2)$ we have allowed for soft breaking of Z'_2 in order to preserve the chance of CP violation in the potential while we do not allow for any breaking of Z_2 in order to have a stable lightest component of η as a DM candidate. Note that, as a consequence of the unbroken Z_2 , there is no mixing in mass terms between $\Phi_{1,2}$ and η . It is worth realizing that, since η does not couple to quarks, there are no constraints on the charged inert Higgs mass from the $b \rightarrow s\gamma$ decay.

B. 2HDM mass eigenstates

In the (noninert) 2HDM sector of the model, we denote the doublets (in a basis where both have a vacuum expectation value [VEV])

$$\begin{aligned} \Phi_1 = & \begin{pmatrix} \varphi_1^+ \\ (v_1 + \eta_1 + i\chi_1)/\sqrt{2} \end{pmatrix}, \\ \Phi_2 = & \begin{pmatrix} \varphi_2^+ \\ (v_2 + \eta_2 + i\chi_2)/\sqrt{2} \end{pmatrix}, \end{aligned} \quad (2.6)$$

and adopt the mixing matrix R , defined by

$$\begin{pmatrix} H_1 \\ H_2 \\ H_3 \end{pmatrix} = R \begin{pmatrix} \eta_1 \\ \eta_2 \\ \eta_3 \end{pmatrix}, \quad (2.7)$$

satisfying

$$R\mathcal{M}^2R^T = \mathcal{M}_{\text{diag}}^2 = \text{diag}(M_1^2, M_2^2, M_3^2), \quad (2.8)$$

and parametrized in terms of three rotation angles α_i as

$$R = \begin{pmatrix} c_1c_2 & s_1c_2 & s_2 \\ -(c_1s_2s_3 + s_1c_3) & c_1c_3 - s_1s_2s_3 & c_2s_3 \\ -c_1s_2c_3 + s_1s_3 & -(c_1s_3 + s_1s_2c_3) & c_2c_3 \end{pmatrix} \quad (2.9)$$

with $c_i = \cos\alpha_i$, $s_i = \sin\alpha_i$. In Eq. (2.7), $\eta_3 \equiv -\sin\beta\chi_1 + \cos\beta\chi_2$ is the combination of χ_i 's which is orthogonal to the neutral Nambu-Goldstone boson. Here, $\tan\beta \equiv v_2/v_1$.

We also define a mass parameter $\mu^2 \equiv (v^2/2v_1v_2)\text{Re}m_{12}^2$, and note the following useful relation:

$$\text{Im}m_{12}^2 = \text{Im}\lambda_5v_1v_2. \quad (2.10)$$

C. Inert-sector mass eigenstates

Components of the inert doublet are defined as follows:

$$\eta = \begin{pmatrix} \eta^+ \\ (S + iA)/\sqrt{2} \end{pmatrix}. \quad (2.11)$$

The masses of the inert scalars will be given by expressions analogous to those of [6,9]:

$$\begin{aligned} M_{\eta^\pm}^2 &= m_\eta^2 + \frac{1}{2}\Delta_{\text{ch}}^2, \\ M_S^2 &= m_\eta^2 + \frac{1}{2}[\Delta_{\text{ch}}^2 + \Delta_0^2 + \Delta_{\text{split}}^2], \\ M_A^2 &= m_\eta^2 + \frac{1}{2}[\Delta_{\text{ch}}^2 + \Delta_0^2 - \Delta_{\text{split}}^2], \end{aligned} \quad (2.12)$$

where we have introduced the abbreviations

$$\begin{aligned} \Delta_{\text{ch}}^2 &= \lambda_{1133}v_1^2 + \lambda_{2233}v_2^2, & \Delta_0^2 &= \lambda_{1331}v_1^2 + \lambda_{2332}v_2^2, \\ \Delta_{\text{split}}^2 &= \text{Re}\lambda_{1313}v_1^2 + \text{Re}\lambda_{2323}v_2^2. \end{aligned} \quad (2.13)$$

Adopting the simplifying assumptions (denoted ‘‘dark democracy’’)

$$\begin{aligned} \lambda_a \equiv \lambda_{1133} &= \lambda_{2233}, & \lambda_b \equiv \lambda_{1331} &= \lambda_{2332}, \\ \lambda_c \equiv \lambda_{1313} &= \lambda_{2323} \text{ (real)}, \end{aligned} \quad (2.14)$$

the masses can be written as

$$\begin{aligned} M_{\eta^\pm}^2 &= m_\eta^2 + \frac{1}{2}\lambda_a v^2, \\ M_S^2 &= m_\eta^2 + \frac{1}{2}(\lambda_a + \lambda_b + \lambda_c)v^2 \\ &= M_{\eta^\pm}^2 + \frac{1}{2}(\lambda_b + \lambda_c)v^2, \\ M_A^2 &= m_\eta^2 + \frac{1}{2}(\lambda_a + \lambda_b - \lambda_c)v^2 \\ &= M_{\eta^\pm}^2 + \frac{1}{2}(\lambda_b - \lambda_c)v^2. \end{aligned} \quad (2.15)$$

As a consequence of the assumptions (2.14), there are no trilinear couplings $H^\pm\eta^\mp S$ or $H^\pm\eta^\mp A$.

D. Stability of the potential

The condition for positivity of V is discussed in Appendix A for the general potential, Eq. (2.1). In our numerical applications we will limit ourselves to the case of dark democracy defined in (2.14). We find that for this special case, Eqs. (A16) and (A32) must be satisfied for positivity. However, we restrict ourselves even further by requiring V_{12} , V_3 , and V_{123} separately to be positive. Then, in addition to the familiar constraint on V_{12} [7,10,11] and V_3 , we obtain the following condition:

$$\lambda_a \geq \max(0, -2\lambda_b, -\lambda_b \pm \lambda_c), \quad (2.16)$$

implying $m_\eta < M_{\eta^\pm}$. This amounts to a strong constraint on the splitting of the inert-sector spectrum, not present in the full treatment of positivity.

The input parameters in the inert sector are defined by specifying scalar masses (M_S, M_A, M_{η^\pm}) together with m_η , so that the quartic couplings λ_a , λ_b and λ_c can be determined via (2.15). Here we will consider cases (the profile 3 is the only exception; see Sec. III B), with masses ordered as follows: $M_S < M_A < M_{\eta^\pm}$. This is motivated by the fact that a positive contribution to the electroweak precision observable T from the inert sector (see Sec. VI) makes it easier to allow for heavy 2HDM masses. For this case it is easy to show that the ordering and the positivity condition (2.16) leave a certain nonempty allowed region in the space of $(\lambda_a, \lambda_b, \lambda_c)$, namely $\lambda_a > 0$, $\lambda_b < 0$, $\lambda_a > 2|\lambda_b|$ together with $\lambda_c < 0$ and $|\lambda_b| > |\lambda_c|$. Then the requirement of having the right amount of dark matter (see next section) imposes additional constraints on the masses (or equivalently on the quartic couplings), resulting in a relatively small region of allowed $(\lambda_a, \lambda_b, \lambda_c)$. If $M_S < M_{\eta^\pm} < M_A$, then the constraints are less tight.

III. BENCHMARKS

In numerical studies we will assume that S is the lightest neutral scalar, $M_S < M_A$. The first profiles have the DM candidate around 75 GeV, a favored value [6,9]. For the heavier neutral partner, we consider a few options at, or slightly above, $M_A = 110$ GeV, which is the lower limit compatible with LEP2 data [12].

In a recent study by Lopez Honorez *et al.* [9], the splitting among inert-sector scalar masses was kept fixed, while a scan over the parameter μ_2 (corresponding to our m_η) and the DM particle mass (M_S in our notation) was performed. In the region of heavy DM particles, a detailed study has also been performed in [13].

We shall instead consider two discrete sets of ‘‘dark’’ profiles, to be specified below. In the first set of dark profiles, we keep the DM particle light. For trial values of the masses and m_η (inspired by the results of [9]), we

estimate the amount of dark matter from micrOMEGAs 2.2 [14,15], in the IDM version developed by Lopez Honorez *et al.* [9]. That version has only *one* Z_2 -even doublet, whereas we here consider two such doublets, Φ_1 and Φ_2 (with many more “free” parameters). Therefore the calculation of amplitudes for various DM annihilation channels is more complicated.

The mass of the charged partner, M_{η^\pm} , and the inert-sector mass parameter m_η have been chosen such that a reasonable amount of dark matter is obtained for at least one set of the parameters (3.6). In the context of dark matter, the parameter m_η is important, since a particular choice for the inert neutral scalar masses M_S and M_A together with m_η constrain $(\lambda_a, \lambda_b, \lambda_c)$ which, in turn, are responsible for the annihilation of dark matter into the visible sector; see [9]. In the original IDM, the essential parameter determining the trilinear coupling among two DM particles and the SM Higgs boson, is

$$\lambda_L \equiv \frac{1}{2}(\lambda_a + \lambda_b + \lambda_c). \quad (3.1)$$

In the present model, the trilinear coupling between two S particles and a neutral-Higgs boson is determined by

$$\lambda_L(v_1\eta_1 + v_2\eta_2)SS. \quad (3.2)$$

Projecting out the coupling to a particular neutral-Higgs boson, we find

$$SSH_j: F_{SSj}\lambda_L, \quad \text{with} \quad F_{SSj} = \cos\beta R_{j1} + \sin\beta R_{j2}, \quad (3.3)$$

where the prefactor satisfies $|F_{SSj}| \leq 1$, since R is unitary. In particular, $F_{SS1} = \cos(\beta - \alpha_1)\cos\alpha_2$.

Similarly, the four-point coupling involving two S particles and two neutral-Higgs bosons is determined by

$$\frac{1}{4}[(\lambda_a + \lambda_b + \lambda_c)(\eta_1^2 + \eta_2^2) + (\lambda_a + \lambda_b - \lambda_c)(\chi_1^2 + \chi_2^2)]SS. \quad (3.4)$$

Projecting out the coupling to the lightest Higgs boson, we find

$$SSH_1H_1: \frac{1}{2}(\lambda_L - \lambda_c R_{13}^2) = \frac{1}{2}(\lambda_L - \lambda_c \sin^2\alpha_2). \quad (3.5)$$

In our estimates of the DM density, we shall follow the approach of [9], taking λ_L as the relevant parameter. The DM values presented in this work are based on the full tree-level calculation performed using micrOMEGAs 2.2 with all intermediate and final states originating from the rich 2HDM structure of the model.²

A. 2HDM masses

For each of the dark profiles, we consider the following mass parameters of the (noninert) 2HDM sector:

$$\text{Set A: } (M_1, M_2) = (100, 300) \text{ GeV}, \quad \mu = 200 \text{ GeV}, \quad (3.6a)$$

$$\text{Set B: } (M_1, M_2) = (200, 400) \text{ GeV}, \quad \mu = 400 \text{ GeV}, \quad (3.6b)$$

$$\text{Set C: } (M_1, M_2) = (400, 500) \text{ GeV}, \quad \mu = 400 \text{ GeV}. \quad (3.6c)$$

A nonzero value for μ is adopted, in order to accommodate the unitarity constraints limiting quartic couplings. We avoid degeneracy of M_1 and M_2 , since that would be a source of potential difficulties to produce CP violation; see Sec. V C for a detailed discussion.

B. Light DM particle

We shall consider the following “light” DM profiles:

Profile 1: $M_S = 75$ GeV,	$M_A = 110$ GeV,	$M_{\eta^\pm} = 112$ GeV,	(3.7)
Profile 1': $M_S = 77$ GeV,	$M_A = 110$ GeV,	$M_{\eta^\pm} = 112$ GeV,	
Profile 2: $M_S = 75$ GeV,	$M_A = 120$ GeV,	$M_{\eta^\pm} = 125$ GeV,	
Profile 3: $M_S = 75$ GeV,	$M_A = 120$ GeV,	$M_{\eta^\pm} = 85$ GeV,	
Profile 4: $M_S = 100$ GeV,	$M_A = 110$ GeV,	$M_{\eta^\pm} = 115$ GeV,	
Profile 5: $M_S = 120$ GeV,	$M_A = 125$ GeV,	$M_{\eta^\pm} = 130$ GeV.	

C. Heavier DM particle

We also consider some profiles where the two neutral inert-particle masses are higher, and rather close, another domain favored by [9]:

²Within the approximate treatment of positivity, and keeping only the lowest mass state of the 2HDM, the full result can be mimicked by an appropriate tuning of m_η , which in turn amounts to a tuning of λ_a .

$$\begin{aligned}
 \text{Profile 11: } M_S &= 500 \text{ GeV}, & M_A &= 501 \text{ GeV}, & M_{\eta^\pm} &= 502 \text{ GeV}, \\
 \text{Profile 12: } M_S &= 600 \text{ GeV}, & M_A &= 601 \text{ GeV}, & M_{\eta^\pm} &= 602 \text{ GeV}, \\
 \text{Profile 13: } M_S &= 800 \text{ GeV}, & M_A &= 802 \text{ GeV}, & M_{\eta^\pm} &= 804 \text{ GeV}, \\
 \text{Profile 14: } M_S &= 1000 \text{ GeV}, & M_A &= 1002 \text{ GeV}, & M_{\eta^\pm} &= 1005 \text{ GeV}.
 \end{aligned} \tag{3.8}$$

The latter profiles have a high degree of degeneracy among the masses. This is required in order to have the correct amount of dark matter, but will also minimize the contribution to the electroweak observable T . For a detailed study of the IDM in the high-mass regime, see [13].

IV. SEARCH STRATEGY

In general, our goal will be to verify that within the IDM2 model one can accommodate the following features:

- (i) a ‘‘heavy’’ lightest neutral scalar (so that the naturalness problem is alleviated),
- (ii) at least one neutral scalar odd under Z_2 consistent with the present limits on the DM abundance,
- (iii) CP violation in the potential (introduced via m_{12}^2 and λ_5).

First we choose the following input parameters for the 2HDM: $\tan\beta$, M_1 , M_2 , M_{H^\pm} , and μ , together with $(\alpha_1, \alpha_2, \alpha_3)$. All remaining parameters of the 2HDM sector are calculable in terms of those chosen above [16] (see also [17]). For the inert sector we choose $M_S \sim 70\text{--}80$ GeV or ≥ 500 GeV (DM candidate), M_A , M_{η^\pm} , and m_η (needed for determination of relevant quartic couplings in V_{123} which are necessary for calculating the DM abundance).

Then the following strategy will be applied while determining allowed regions in the parameter space of the model:

- (1) We fix $\tan\beta$, M_{H^\pm} , sets of 2HDM masses (M_1, M_2, μ), and profiles of the inert-sector parameters (dark profiles M_S, M_A, M_{η^\pm}).
- (2) Next we check if, for a given choice of dark profile (M_S, M_A, M_{η^\pm}) and (M_1, M_2, μ), there exists a value of m_η such that the model predicts the right order of magnitude for the dark matter abundance.
- (3) Then we scan over the mixing angles $(\alpha_1, \alpha_2, \alpha_3)$ of the 2HDM, requiring that:
 - (a) The naturalness is alleviated for each Higgs boson

$$\frac{|\delta M^2|}{M^2} = |\alpha_i| \frac{\Lambda^2}{M^2} < D, \tag{4.1}$$

where M denotes a generic Higgs boson mass, δM^2 stands for the top-quark contribution to the one-loop correction to M^2 , α_i is a calculable coefficient in terms of the mixing angles, etc. The cutoff should be chosen to be in the TeV region, e.g. modestly $\Lambda \simeq 2$ TeV. The fine-tuning parameter D is to be chosen according to our aesthetic standards.

- (b) Based on the experience gained from [6] we restrict the scan to heavy (≥ 100 GeV) Higgs bosons in the

2HDM sector (so that the little hierarchy problem could be that way reduced, that would be an analog of the heavy SM Higgs of [6]). It is worth noting that here some possible tension between parameters emerges. It may appear as we increase Higgs masses in the 2HDM sector trying to retain small quartic constants. Even though the masses could be raised by increasing $\mu^2 \sim m_{12}^2$ in the potential, nevertheless the mass of one scalar would still remain $\sim v$ (see e.g. [18]). In order to increase its mass some combination of quartic couplings in V_{12} will have to be large, therefore checking the unitarity in the 2HDM sector is essential to guarantee that λ_i 's remain in a perturbative regime.

- (c) Remaining experimental constraints are satisfied.
- (d) CP is violated, i.e. α_i are far enough from their CP conserving limits. We use the invariants J_i , $i = 1, 2, 3$ [19] as a measure of CP violation. Eventually we plot an average and/or maximum (with respect to the mixing angles α_i) for $|\text{Im}J_1|$ and the electron electric dipole moment (EDM) to illustrate the strength of CP violation.

V. THEORETICAL CONSTRAINTS

A. The little hierarchy

As an order-of-magnitude estimate for radiative corrections to neutral-Higgs boson masses, we consider the contributions that arise from top-quark loops:

$$\delta M_j^2 = -\frac{3m_t^2}{4\pi^2 v^2} \Lambda_j^2 (a_j^2 + \tilde{a}_j^2) \quad \text{for } j = 1, 2, 3, \tag{5.1}$$

where a_j and \tilde{a}_j are defined in (3.21) of [20]:

$$a_j \equiv \frac{R_{j2}}{s_\beta}, \quad \tilde{a}_j \equiv -\frac{c_\beta R_{j3}}{s_\beta}. \tag{5.2}$$

Similarly, for the charged-Higgs particles we find

$$\delta M_{H^\pm}^2 = -\frac{3m_t^2}{4\pi^2 v^2} \Lambda_{H^\pm}^2 \cot^2 \beta. \tag{5.3}$$

Since the inert doublet does not couple to fermions there is no hierarchy problem for S and A .

We adopt the following simple condition:

$$\frac{|\delta M_j^2|}{M_j^2} < D, \quad \frac{|\delta M_{H^\pm}^2|}{M_{H^\pm}^2} < D \tag{5.4}$$

with the amount of fine-tuning parametrized by D . For the resulting cutoff we will choose

$$\Lambda = \min(\Lambda_j, \Lambda_{H^\pm}). \quad (5.5)$$

This quantity Λ will in general be most constrained by the value of M_1 (unless when $a_1^2 + \tilde{a}_1^2$ is small). For an alleviation of the hierarchy problem, we would like to have Λ large compared to the Higgs masses.

B. Perturbativity and unitarity

To preserve perturbativity we shall impose the following conditions on quartic and Yukawa couplings of neutral- and charged-Higgs bosons

$$\lambda_i, \frac{\sqrt{2}m_t}{v}|a_j|, \frac{\sqrt{2}m_t}{v}|\tilde{a}_j|, \frac{m_t}{\sqrt{2}v} \cot\beta, \lambda_a, \lambda_b, \lambda_c < 4\pi. \quad (5.6)$$

Since we will consider $\tan\beta \geq 0.5$, the last three conditions will always be satisfied. We also impose unitarity on the Higgs-Higgs scattering amplitudes [21–23].

C. CP violation

Since our intention here is to outline a model which would possess CP violation in the Higgs potential we shall discuss this issue in more detail. The magnitude of CP violation can be quantified in terms of the invariants introduced by Lavoura and Silva [19]. However here we prefer to adopt the more general, basis-independent approach of Gunion and Haber and calculate the invariants J_1, J_2 , and J_3 of [24]. They state (theorem 4) that the Higgs sector is CP -conserving if and only if all J_i are real. The calculations of these quantities are straightforward, and we end up with the following result, valid for our choice of basis:

$$\text{Im}J_1 = -\frac{v_1^2 v_2^2}{v^4}(\lambda_1 - \lambda_2) \text{Im}\lambda_5, \quad (5.7)$$

$$\begin{aligned} \text{Im}J_2 = & -\frac{v_1^2 v_2^2}{v^8} [((\lambda_1 - \lambda_3 - \lambda_4)^2 - |\lambda_5|^2)v_1^4 \\ & + 2(\lambda_1 - \lambda_2) \text{Re}\lambda_5 v_1^2 v_2^2 - ((\lambda_2 - \lambda_3 - \lambda_4)^2 \\ & - |\lambda_5|^2)v_2^4] \text{Im}\lambda_5, \end{aligned} \quad (5.8)$$

$$\text{Im}J_3 = \frac{v_1^2 v_2^2}{v^4}(\lambda_1 - \lambda_2)(\lambda_1 + \lambda_2 + 2\lambda_4) \text{Im}\lambda_5. \quad (5.9)$$

We note that since we have chosen a basis with real VEV's, there is no CP violation when $\text{Im}\lambda_5 = 0$ (it should be realized that $\text{Im}m_{12}^2$ and $\text{Im}\lambda_5$ are not independent here; see (2.10)). Then an interesting question arises: Is it possible for $\text{Im}\lambda_5 \neq 0$ to have no CP violation? It turns out that the answer is “yes,” as will be discussed in the following.

The simultaneous vanishing of the three $\text{Im}J_i$ implies that CP is conserved. This can happen for five distinct cases:

- (i) *Case A*: $\text{Im}\lambda_5 \neq 0$ with $v_1 = 0$ ($\tan\beta \rightarrow \infty$).
- (ii) *Case B*: $\text{Im}\lambda_5 \neq 0$ with $v_2 = 0$ ($\tan\beta = 0$).

- (iii) *Case C*: $\text{Im}\lambda_5 = 0$. This corresponds to \mathcal{M}^2 [see (2.8)] being block diagonal, and the diagonalization performed in terms of only *one* rotation angle.
- (iv) *Case D*: $\text{Im}\lambda_5 \neq 0$ with $\lambda_1 = \lambda_2$ and $v_1 = v_2$.
- (v) *Case E*: $\text{Im}\lambda_5 \neq 0$ with $\lambda_1 = \lambda_2$, $v_1 \neq v_2$ and $(\lambda_1 - \lambda_3 - \lambda_4)^2 = |\lambda_5|^2$.

Some comments are here in order (details are discussed in Appendix B):

- (i) When all three masses are degenerate, CP is conserved because $\text{Im}\lambda_5 = 0$. This corresponds to case C.
- (ii) When there is only partial mass degeneracy, $M_1 = M_2 < M_3$ or $M_1 < M_2 = M_3$, there are instances of CP conservation corresponding to cases C, D, and E.
- (iii) There are also instances of CP conservation in the mass nondegenerate case $M_1 < M_2 < M_3$ corresponding to cases C, D, and E.

The above discussion shows that, in terms of our input parameters [$\tan\beta, M_1, M_2, M_{H^\pm}$, and μ , together with $(\alpha_1, \alpha_2, \alpha_3)$] there exist various nontrivial locations such that CP is conserved even though $\text{Im}\lambda_5 \neq 0$ (the case of $\text{Im}\lambda_5 = 0$ is relatively obvious). Since our intention is to build a model that allows for a substantial amount of CP violation, we would like to show regions of parameter space where that indeed happens. However, in light of the above discussion, the determination of such locations cannot easily be performed analytically.

The chance for successful electroweak baryogenesis is the crucial motivation for our discussion of CP violation. However, without a dedicated analysis of baryogenesis (which is beyond the scope of this project) it is hard to estimate the amount of CP violation that is necessary. Therefore, we have adopted the following strategy to illustrate the strength of CP violation *which is available* in the model. We plot both the electron electric dipole moment d_e and the invariant $|\text{Im}J_1|$ (which are physical quantities) in the region of the parameter space allowed by all the other constraints. In order to estimate the amount of potential CP violation we show both averaged and maximal values of d_e and $|\text{Im}J_1|$ (the choice of J_1 (as opposed to J_2 and J_3) is arbitrary, however we recall that it is sufficient for CP violation to have just one of the J_i complex). Large splitting between averaged and maximal values indicates the potential for CP violation hidden in the appropriate choice of mixing angles α_i . Of course, in a realistic situation (having the prediction for electroweak baryogenesis within the model) we would need to have d_e below the experimental upper limit and nevertheless enough CP violation for successful baryogenesis.

In Appendix B, in Figs. 7 and 8, we show how allowed regions in the $(\alpha_1, \alpha_2, \alpha_3)$ space are distributed.

VI. EXPERIMENTAL CONSTRAINTS

We here review various experimental constraints that will be imposed on the model.

T and S .—We adopt the results from [25,26] in order to calculate T and S within our model. Since for the Higgs fields we will use a basis in which only Φ_1 has nonzero VEV (the so-called Higgs basis) some necessary transformations must be performed; see Appendix C for details. For the model discussed here the rotation matrix O defined by Eq. (59) of [25] reads

$$O = \begin{pmatrix} O_{11} & O_{12} & O_{13} & 0 & 0 \\ O_{21} & O_{22} & O_{23} & 0 & 0 \\ O_{31} & O_{32} & O_{33} & 0 & 0 \\ 0 & 0 & 0 & 1 & 0 \\ 0 & 0 & 0 & 0 & 1 \end{pmatrix} \quad (6.1)$$

and the mixing matrix V of that paper becomes

$$V = \begin{pmatrix} i & O_{11} & O_{12} & O_{13} & 0 & 0 \\ 0 & O_{21} + iO_{31} & O_{22} + iO_{32} & O_{23} + iO_{33} & 0 & 0 \\ 0 & 0 & 0 & 0 & 1 & i \end{pmatrix}, \quad (6.2)$$

with $U = \mathbf{1}$. Therefore, $U^\dagger V = V$, and

$$V^\dagger V = \begin{pmatrix} 1 & -iO_{11} & -iO_{12} & -iO_{13} & 0 & 0 \\ iO_{11} & 1 & iO_{13} & -iO_{12} & 0 & 0 \\ iO_{12} & -iO_{13} & 1 & iO_{11} & 0 & 0 \\ iO_{13} & iO_{12} & -iO_{11} & 1 & 0 & 0 \\ 0 & 0 & 0 & 0 & 1 & i \\ 0 & 0 & 0 & 0 & -i & 1 \end{pmatrix}. \quad (6.3)$$

Since this is block diagonal, the contribution to T (and to S) from the inert doublet is additive (the inert fields must always appear in pairs, there is no interference between the “visible” and the inert sector at the one-loop order):

$$T = T_{2\text{HDM}} + \frac{1}{16\pi\sin^2\theta_W m_W^2} [F(M_{\eta^\pm}^2, M_S^2) + F(M_{\eta^\pm}^2, M_A^2) - F(M_A^2, M_S^2)], \quad (6.4)$$

where $\alpha_{\text{e.m.}} T_{2\text{HDM}} = \Delta\rho_{2\text{HDM}}$ is given by (63) of [25]. In our case, the matrices (C3) and (C6) should be adopted. Similarly, S can be obtained from the results given in [26]. We impose the bounds $|\Delta T| < 0.10$, $|\Delta S| < 0.10$ [27], at the 1- σ level.

We note that T , which is our main concern, gets a positive contribution from a splitting between the masses of charged and neutral-Higgs bosons, whereas a pair of neutral ones gives a negative contribution. In fact, since the function F is symmetric in its two arguments, these two opposite-sign contributions cancel in the limit when the charged boson is degenerate with either of the two neutral ones.

$B_0 - \bar{B}_0$ mixing.—Because of the possibility of charged-Higgs exchange, in addition to W^\pm exchange, the $B_0 - \bar{B}_0$ mixing constraint excludes low values of $\tan\beta$ and low values of M_{H^\pm} [28–30]. Here we follow the procedure of [31].

$B \rightarrow X_s \gamma$: The $b \rightarrow s \gamma$ transition may also proceed via charged-Higgs exchange, so some regions of the parameter space with low values of $\tan\beta$ and M_{H^\pm} are excluded. The exact region of exclusion is sensitive to higher-order QCD effects [32–35], and roughly excludes $M_{H^\pm} < 300$ GeV. Again, we follow the approach of [31].

$B \rightarrow \tau \bar{\nu}_\tau X$.—The charged-Higgs contribution may substantially modify the branching ratio for $B \rightarrow \tau \bar{\nu}_\tau X$ [36]. The measurement [37] of $\mathcal{B}(B \rightarrow \tau \bar{\nu}_\tau X)$ leads to the following constraint:

$$\frac{\tan\beta}{M_{H^\pm}} < 0.53 \text{ GeV}^{-1} \quad (6.5)$$

at 95% CL. This is in fact a very weak constraint. A more recent measurement gives $\mathcal{B}(B^- \rightarrow \tau \bar{\nu}_\tau) = (1.79 \pm 0.71) \times 10^{-4}$ [38], where we have added in quadrature symmetrized statistical and systematic errors. With the SM prediction of $(1.59 \pm 0.40) \times 10^{-4}$,

$$r_{H\text{exp}} = \frac{\mathcal{B}(B^- \rightarrow \tau \bar{\nu}_\tau)}{\mathcal{B}(B^- \rightarrow \tau \bar{\nu}_\tau)_{\text{SM}}} = 1.13 \pm 0.53. \quad (6.6)$$

Within the framework of the 2HDM, one finds [39]

$$r_{H2\text{HDM}} = \left[1 - \frac{m_B^2}{M_{H^\pm}^2} \tan^2\beta \right]^2. \quad (6.7)$$

Then the data imply that two sectors at large values of $\tan\beta$ and low values of M_{H^\pm} are excluded.

$B \rightarrow D\tau\bar{\nu}_\tau$.—Measurements [40] of the ratio

$$R^{\text{exp}} = \frac{\mathcal{B}(B \rightarrow D\tau\nu_\tau)}{\mathcal{B}(B \rightarrow D\ell\nu_\ell)}, \quad \ell = e, \mu, \quad (6.8)$$

can also be used to constrain the coupling of the charged Higgs to the τ , more precisely $\tan\beta/M_{H^\pm}$. It thus restricts large values of $\tan\beta$ and low values of M_{H^\pm} [41], in a region of parameter space similar to the one following from $B \rightarrow \tau \bar{\nu}_\tau X$, but is considerably stronger.

$LEP2$ nondiscovery.—The nondiscovery of a Higgs boson at LEP2 imposes a bound on how strongly the lightest one can couple to the Z and to $b\bar{b}$. Useful results for this constraint are available in table 27 of [42]. Adopting the standard notation

$$\sigma_{Z(H \rightarrow b\bar{b})} = \sigma_{Z(H \rightarrow b\bar{b})}^{\text{SM}} \times C_{Z(H \rightarrow b\bar{b})}^2 \quad (6.9)$$

one can approximately parametrize the upper limit on $C_{Z(H \rightarrow b\bar{b})}^2$ from the table as follows:

$$C_{Z(H \rightarrow b\bar{b})}^2 \leq \begin{cases} 0.05 & \text{for } 12 \text{ GeV} < M_A \leq 80 \text{ GeV}, \\ 0.1 & \text{for } 80 \text{ GeV} < M_A \leq 90 \text{ GeV}, \\ 0.2 & \text{for } 90 \text{ GeV} < M_A < 110 \text{ GeV}. \end{cases} \quad (6.10)$$

For $e^+e^- \rightarrow ZH_1$ the coefficient $C_{Z(H \rightarrow b\bar{b})}^2$ is given by (4.3) of [20]:

$$C_{Z(H_1 \rightarrow b\bar{b})}^2 = (c_\beta R_{11} + s_\beta R_{12})^2 \frac{1}{c_\beta^2} (R_{11}^2 + s_\beta^2 R_{13}^2). \quad (6.11)$$

Then the constraint (6.10) limits the parameter space.

R_b .—The branching ratio for $Z \rightarrow b\bar{b}$ is also affected by Higgs exchange. As noticed in [20], the contributions from neutral-Higgs bosons to R_b are negligible, however, charged-Higgs boson contributions, as given by [43], Eq. (4.2), exclude low values of $\tan\beta$ and low M_{H^\pm} . Experimentally $R_b \equiv \Gamma_{Z \rightarrow b\bar{b}}/\Gamma_{Z \rightarrow \text{had}} = 0.21629 \pm 0.00066$ [27]. It is easy to see that the correction $\delta\Gamma_{Z \rightarrow b\bar{b}}$ implies the following change for R_b :

$$\delta R_b = \frac{\delta\Gamma_{Z \rightarrow b\bar{b}}}{\Gamma_{Z \rightarrow \text{had}}} (1 - R_b), \quad (6.12)$$

where $\Gamma_{Z \rightarrow \text{had}} = (1.7444 \pm 0.0020) \text{ GeV}$ [27]. Since $\delta\Gamma_{Z \rightarrow b\bar{b}}$ is known within the 2HDM [43], so is δR_b . We require

$$\delta R_b < 0.00066, \quad (6.13)$$

corresponding to $\delta\Gamma_{Z \rightarrow b\bar{b}} = 1.47 \text{ MeV}$ at the $1\text{-}\sigma$ level.

Muon anomalous magnetic moment.—Since here we are considering heavy Higgs bosons ($M_i \gtrsim 100 \text{ GeV}$) therefore, according to [31,44], the 2HDM contribution to the muon anomalous magnetic moment is negligible even for $\tan\beta$ as large as ~ 40 .

Electron electric dipole moment.—The bounds on electric dipole moments constrain the allowed amount of CP violation of the model. We adopt the bound [45] (see also [46])

$$|d_e| \lesssim 1 \times 10^{-27} [e \text{ cm}], \quad (6.14)$$

at the $1\text{-}\sigma$ level. The contribution due to neutral-Higgs exchange,³ via the two-loop Barr-Zee effect [48], is given by Eq. (3.2) of [46] in terms of the neutral-sector mixing matrix O , defined in [49], and related to our R via

$$\begin{pmatrix} O_{11} & O_{12} & O_{13} \\ O_{21} & O_{22} & O_{23} \\ O_{31} & O_{32} & O_{33} \end{pmatrix} = \begin{pmatrix} R_{33} & R_{23} & R_{13} \\ R_{31} & R_{21} & R_{11} \\ R_{32} & R_{22} & R_{12} \end{pmatrix}. \quad (6.15)$$

This rotation matrix O should not be confused with the one appearing in Eq. (6.1).

VII. RESULTS

Subject to the limitations discussed above, we may now scan over the parameter space, imposing the constraint

$$\chi^2 = \sum \chi_i^2 < 5.99, \quad 95\% \text{CL}, \quad (7.1)$$

as appropriate for identifying allowed regions in two di-

³Neglecting the Cabibbo-Kobayashi-Maskawa (CKM) mixing, the charged-Higgs contribution to d_e vanishes in the 2HDM (with softly broken Z_2) up to two loops [47].

mensions, $(\tan\beta, M_{H^\pm})$. The sum runs over all the experimental constraints discussed above.

Our results will be given in terms of contour plots of various quantities of interest. Regions corresponding to values being confined within certain intervals are indicated by a color coding as indicated. The external contour shows the maximal region consistent with the experimental and theoretical constraints we adopt (i.e., without the naturalness condition imposed on Λ/\sqrt{D} , unless explicitly stated).

The model discussed here contains many parameters (masses, mixing angles, etc.). In projecting down our results to a lower-dimensional space, we have decided to favor the more ‘‘physical’’ parameters $\tan\beta$ and M_{H^\pm} together with neutral scalar masses (and μ). In this section, most of the plots show (for fixed inert masses, M_S, M_A, M_{η^\pm} , fixed 2HDM neutral masses, M_1, M_2 , and μ) allowed regions in the $(\tan\beta, M_{H^\pm})$ space. The remaining parameters, the neutral-Higgs-sector mixing angles, α_1, α_2 , and α_3 , which are not specified in those plots, have been averaged over, or a maximum has been extracted. Thus, for each allowed point in $(\tan\beta, M_{H^\pm})$ there exist α ’s such that all constraints are satisfied.

A. Light dark matter particle

We first consider the set of dark profiles for which the DM particle is light, at $\sim 75 \text{ GeV}$; see Eq. (3.7). These profiles may be compared with the parameters considered by Lopez Honorez *et al.* [9], in their Fig. 5, where it was shown that the correct amount of dark matter may be obtained with dark-matter mass of the order of 50–80 GeV, for splittings of the order 10–50 GeV.

In Table I we summarize the results for the DM density Ωh^2 for the different combinations of dark profiles of Eq. (3.7), and non-inert-sector parameters of Eq. (3.6). These are obtained from running micrOMEGAs [14,15], as described in Sec. III. For the quartic couplings in the inert sector (denoted here by $\lambda_\eta/2$), we use the value 0.1 (the amount of dark matter is practically independent of this coupling [9]). Here, ‘‘OK’’ means that a value within 3σ of the WMAP value 0.1131 ± 0.0034 [50], can be found for a suitable choice of m_η . For these profiles of light DM particles, typically values $m_\eta \sim 30\text{--}50 \text{ GeV}$ are required.

Profile 1’ corresponds to the allowed horizontal band in Fig. 9 of Lundström *et al.* [12], in the sense that we find solutions for sets B and C, corresponding to heavier non-inert Higgs particles. This band is rather narrow: for $M_S = 75 \text{ GeV}$ we find too much dark matter, at $M_S = 79 \text{ GeV}$ too little. It appears shifted by a couple of GeV, with respect to the results of [12], presumably due to the use of a different DM code, micrOMEGAs [14,15] vs DARKSUSY [51].

All these profiles (except profile 3) have the charged particle heavier than both the neutral ones, in order that the inert sector makes a positive contribution to T (see

TABLE I. Dark-matter density Ωh^2 for different dark profiles, DP1, DP1', DP3, DP4, DP5 with mass parameters (M_S, M_A, M_{η^\pm}) , and different mass-parameter sets A–C with mass parameters (M_1, M_2, μ) , all in GeV; see Sec. III.

Ωh^2	DP1 (75, 110, 112)	DP1' (77, 110, 112)	DP3 (75, 110, 85)	DP4, DP5 (100, 110, 115)
A (100, 300, 200)	OK	<0.07	<0.09	<0.01
B (200, 400, 400)	>0.24	OK	OK	<0.01
C (400, 500, 400)	>0.24	0.08–0.09	≤ 0.10	<0.01

Sec. VI). This, in turn, allows for a higher value of the “ordinary” neutral-Higgs particle [6] that enters the electroweak fits.

Profiles 4 and 5 give $\Omega h^2 \leq 0.01$ (consistent with Figs. 8 and 9 of [12]) and will not be considered any further.

Dark profile 1.—We start discussing the case $(M_S, M_A, M_{\eta^\pm}) = (75, 110, 112)$ GeV. Among the three sets of mass parameters considered for the visible sector, only set A $(M_1, M_2, \mu) = (100, 300, 200)$ GeV gives a reasonable value of Ωh^2 . With m_η of the order 45–55 GeV we obtain $\Omega h^2 \simeq 0.10$ –0.13. Higher values of m_η yield too high values of Ωh^2 . For profile 1 and sets B and C, the value is too high, $\Omega h^2 \geq 0.24$.⁴ The allowed region is shown in Fig. 1. The figure is obtained by scanning over $\tan\beta$ from 0.5 to 50, and over M_{H^\pm} from 300 GeV (barely above the $B \rightarrow X_s \gamma$ cutoff) to 700 GeV. For each point in the $(\tan\beta, M_{H^\pm})$ plane, a scan over mixing angles $(\alpha_1, \alpha_2, \alpha_3)$ is performed, analyzing all models compliant with the constraints, showing contours of the CP -violating quantity $|\text{Im}J_1|$ and the electron electric dipole moment (EDM). These two quantities provide two different measures of the amount of CP violation. The outer contours delineate the regions within which consistent solutions are found for one or more sets of mixing angles α_i . The averages presented in the left panels are obtained by averaging over all sets of $(\alpha_1, \alpha_2, \alpha_3)$ for which the experimental constraints are satisfied according to Eq. (7.1). Similarly, the maxima in the right panels correspond to maxima of absolute values, obtained from the same scans over allowed sets of $(\alpha_1, \alpha_2, \alpha_3)$.

In the upper part of the figure we display $|\text{Im}J_1|$, while the lower one shows the electron electric dipole moment, $|d_e|$. In the left panels averages over allowed sets of α_i are displayed, while the right ones show extrema. There is no obvious correlation between $|d_e|$ and $|\text{Im}J_1|$, other than both having maxima in the interior of the allowed region.

In Appendix B we discuss the correlations of angles α_i for which viable solutions are found. These are shown separately for small $\tan\beta$ and large $\tan\beta$. In general, it is easier to accommodate CP violation at low values of $\tan\beta$

than at higher values. For high values of $\tan\beta$, the allowed values of these parameters tend to accumulate near the limits where H_2 is odd under CP ($\alpha_2 \simeq 0$, $\alpha_3 \simeq \pm\pi/2$).

For the parameters considered here, $(M_1, M_2, \mu) = (100, 300, 200)$ GeV, the viable models are constrained to $\tan\beta \sim 0.5 - 6$. The cutoff at high $\tan\beta$ is mostly due to the unitarity constraint on the neutral-Higgs sector. We also note a cutoff at $M_{H^\pm} \sim 650$ GeV. This, on the other hand, is due to the electroweak constraints, T in particular.

The fact that the *average* electric dipole moment is rather small compared to the maximum value means that large parts of the $\tan\beta$ - M_{H^\pm} space would remain viable even if the experimental constraint on $|d_e|$ should become significantly tightened.

The little hierarchy.—In this Fig. 1, no constraint from the fine-tuning consideration in Sec. VA is imposed. In Fig. 2 we plot the quantity Λ/\sqrt{D} of Eq. (5.5), which by definition is minimized over the three neutral-Higgs particles and the charged one (for fixed mixing angles α_i). This is next maximized over the α_i (for fixed $\tan\beta$ and M_{H^\pm}) before being plotted in this figure. For the cases considered, we note that Λ/\sqrt{D} reaches up to around 3 TeV. The dominant reason why this varies with $\tan\beta$ and M_{H^\pm} is that the factor

$$\xi_j \equiv a_j^2 + \tilde{a}_j^2 \quad (7.2)$$

of Eq. (5.1), for which solutions are allowed, varies. Specifically, when the factor ξ_1 is small, Λ/\sqrt{D} will be larger. This happens when $\sin\alpha_1 \cos\alpha_2$ and $\cos\beta \sin\alpha_2$ are both small (cf. Appendix B).

Accordingly, imposing the constraint (5.4), with $\Lambda/\sqrt{D} = 2$ TeV, we obtain the more restricted allowed regions shown in Fig. 3. Compared with Fig. 1 (where there is no constraint on Λ), we see a dramatic reduction of the allowed parameter space. For $M_1 = 100$ GeV, only a small region of $M_{H^\pm} \sim 300$ –350 GeV and $\tan\beta \sim 2$ –6 survives. Naturally, this is dominantly caused by the condition (5.4) applied to M_1 .

Dark profile 1'.—This profile has a slightly higher value of M_S , and thus gives allowed models also out to higher values of the noninert Higgs mass, M_1 , corresponding to the horizontal band in Fig. 9 of Ref. [12]. The results for sets B and C are shown in Fig. 4. As compared with profile 1, the heavier S here allows more annihilation to

⁴For sets B and C the lightest 2HDM Higgs is relatively heavy so that SS annihilation via an intermediate H_1 is suppressed, and too much dark matter would survive.

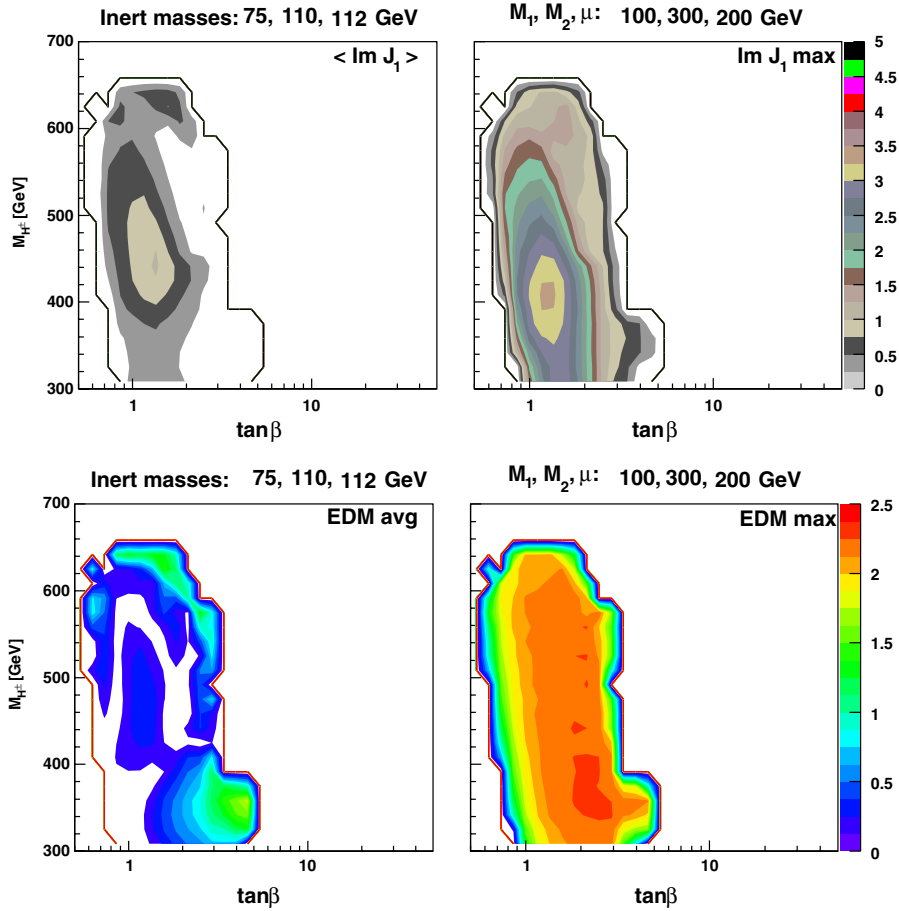


FIG. 1 (color online). Top panels: Relative amount of CP violation. Bottom panels: Electron electric dipole moment in units ($e 10^{-27}$ cm). Left: average. Right: maximum value. Inert-sector masses: (75, 110, 112) GeV. 2HDM-sector masses: $(M_1, M_2, \mu) = (100, 300, 200)$ GeV.

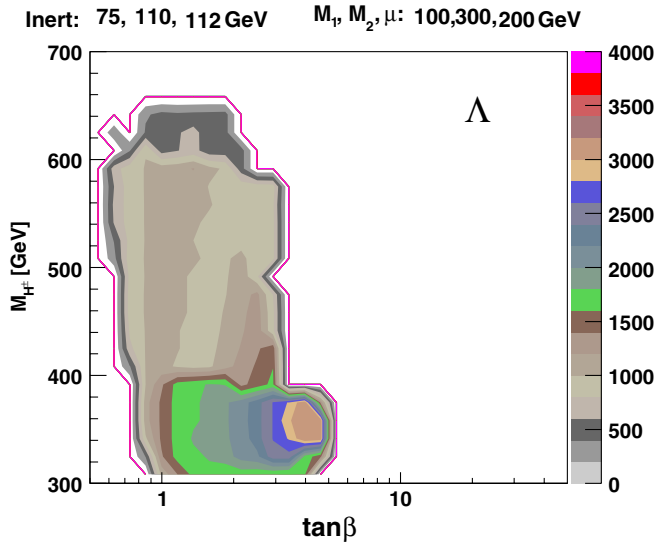


FIG. 2 (color online). Maximum reach in Λ/\sqrt{D} (GeV). Inert-sector masses: (75, 110, 112) GeV. 2HDM-sector masses: $(M_1, M_2, \mu) = (100, 300, 200)$ GeV.

(off-shell) WW pairs, and thus an acceptable value of Ωh^2 can be found.

For set B, there are solutions over most of the explored $\tan\beta$ - M_{H^\pm} plane; for $M_{H^\pm} \sim 400$ – 500 GeV and $M_2 = \mu = 400$ GeV they reach all the way out to $\tan\beta \sim 50$. For set C, on the other hand, the situation is different. Apart from a region around $\tan\beta \sim 1$ – 2 , solutions are only found within two widely separated bands in the $\tan\beta$ - M_{H^\pm} plane. There is one band at $M_{H^\pm} \lesssim 400$ GeV and another at $M_{H^\pm} \lesssim 550$ – 650 GeV, with a region of no solutions in between. This is clearly due to the interplay or partial cancellation of contributions to T , positive from the charged-Higgs boson differing in mass from some neutral ones, and negative from pairs of neutral ones having different masses.

Dark profile 2.—In this case the allowed models are located in essentially the same part of the $\tan\beta$ - M_{H^\pm} plane as for dark profile 1, with similar values for $|\text{Im}J_1|$ and the electron electric dipole moment.

Dark profile 3.—This profile differs from the previous ones in having the charged boson of the inert sector lighter than the heavier neutral one. With this modification from

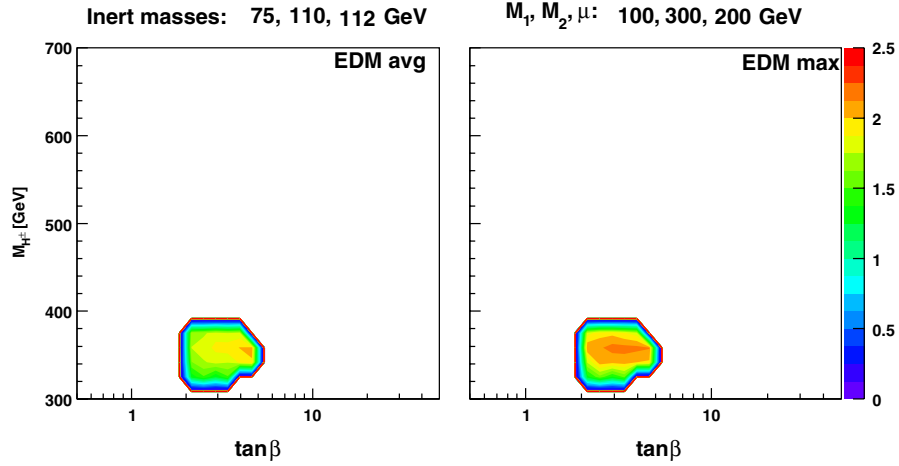


FIG. 3 (color online). Allowed regions for $\Lambda/\sqrt{D} = 2$ TeV (outer contours) and electron electric dipole moment in units ($e 10^{-27}$ cm). Left: average. Right: maximum value. Inert-sector masses: (75, 110, 112) GeV. 2HDM-sector masses: $(M_1, M_2, \mu) = (100, 300, 200)$ GeV.

profile 1, we find acceptable solutions also for heavier Higgs bosons in the noninert sector (sets B and C). The allowed regions in the $\tan\beta$ - M_{H^\pm} plane are quite similar to

those shown in Fig. 4 for profile 1' and also the values of the electric dipole moment are similar.

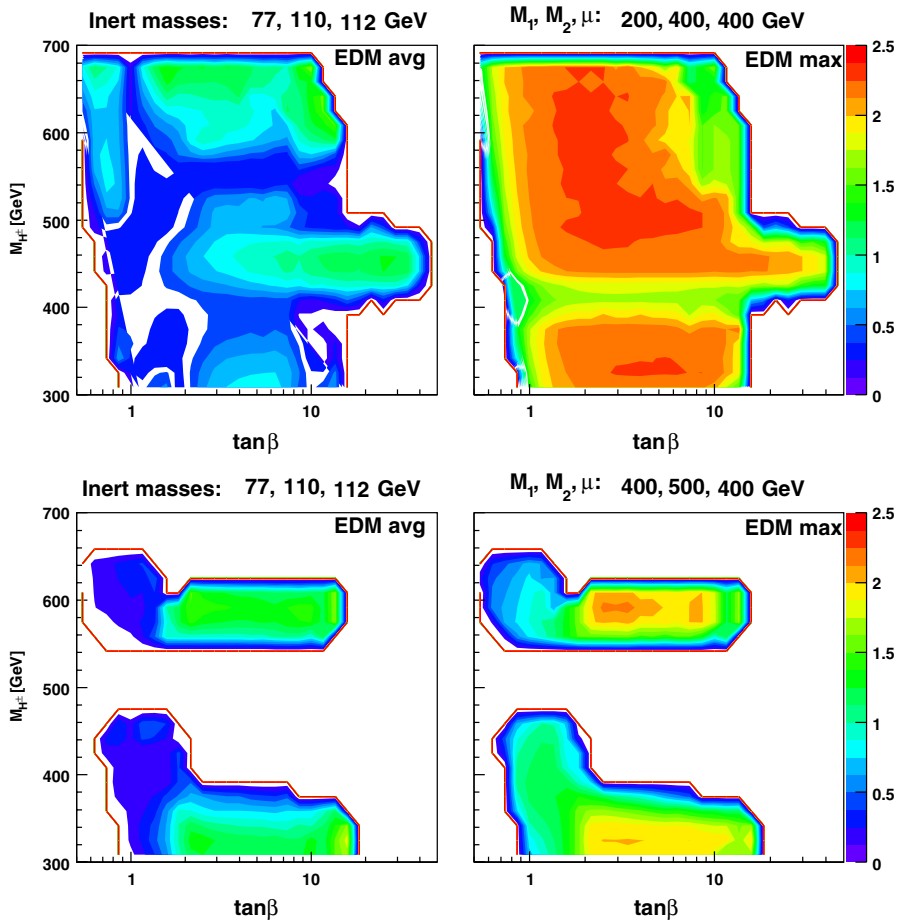


FIG. 4 (color online). Electron electric dipole moment in units ($e 10^{-27}$ cm). Left: average. Right: maximum value. Inert-sector masses: (77, 110, 112) GeV. 2HDM-sector masses: $(M_1, M_2, \mu) = (200, 400, 400)$ GeV and $(400, 500, 400)$ GeV.

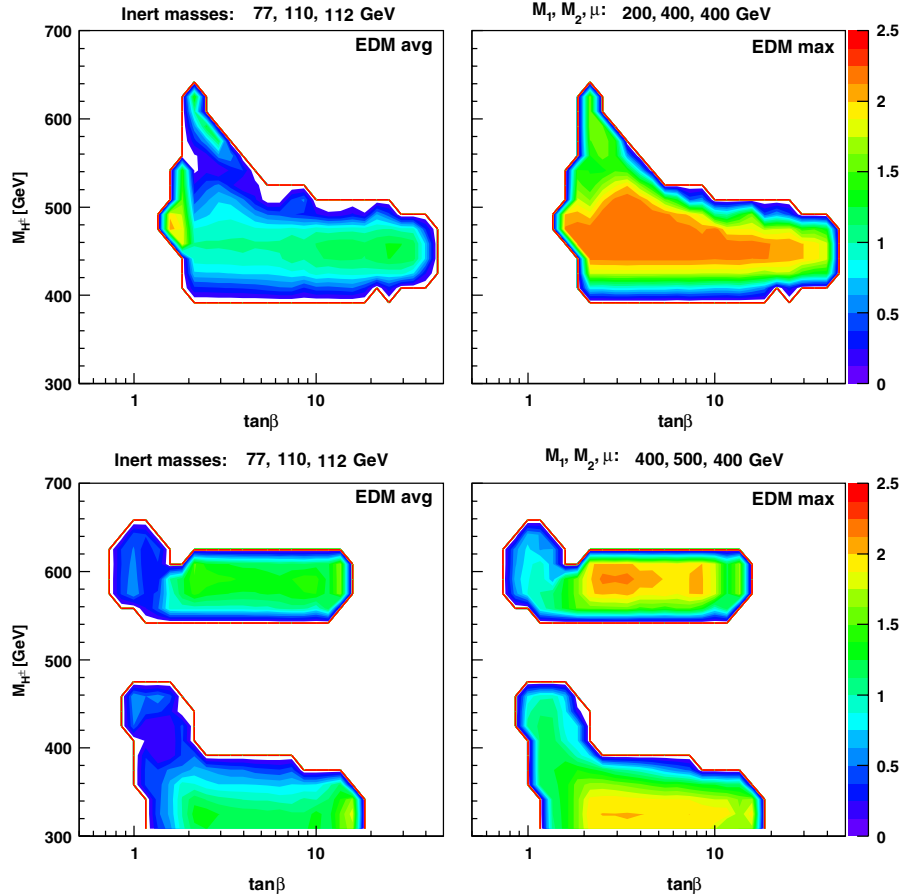


FIG. 5 (color online). Allowed regions for $\Lambda/\sqrt{D} = 2$ TeV (outer contours) and electron electric dipole moment in units ($e 10^{-27}$ cm). Left: average. Right: maximum value. Inert-sector masses: (77, 110, 112) GeV. 2HDM-sector masses: $(M_1, M_2, \mu) = (200, 400, 400)$ GeV and $(400, 500, 400)$ GeV.

The little hierarchy. If we here impose the constraint (5.4), with $\Lambda/\sqrt{D} = 2$ TeV, there is a considerable reduction in the allowed parameter space for set B, whereas for set C essentially the whole parameter space survives, as shown in Fig. 5 for profile 1'.

B. Heavier dark matter particle

The second set of dark profiles has a heavier DM particle. For this case, it was shown (see Fig. 6 of [9]) that the amount of dark matter can satisfy the WMAP constraint [50] provided the splitting in the inert sector is small. We confirm that finding and list in Table II approximate values

of Ωh^2 obtained from micrOMEGAs [14,15] with suitable choices of m_η . The values vary quite a bit with the choice of this parameter. As mentioned above, the small mass splitting in this inert sector also leads to a small (hence acceptable) modification of T .

Dark profiles 11, 12, 13, and 14.—For all these cases, we find solutions for all the three considered sets of noninert mass parameters of Eq. (3.6). The allowed regions in the $\tan\beta$ - M_{H^\pm} plane and the corresponding values for the electron electric dipole moment are very similar to those displayed in Figs. 1 and 4. For set B, with $(M_1, M_2, \mu) = (200, 400, 400)$ GeV, the allowed region extends to large

TABLE II. DM density Ωh^2 for different dark profiles, DP11, DP12, DP13, DP14 with mass parameters (M_S, M_A, M_{η^\pm}) and different 2HDM mass-parameter sets A–C, (M_1, M_2, μ) , all in GeV; see Sec. III.

	DP11 (500, 501, 502)	DP12 (600, 601, 602)	DP13 (800, 802, 804)	DP14 (1000, 1002, 1005)
Ωh^2				
A (100, 300, 200)	≈ 0.09	≈ 0.10	≈ 0.09	≈ 0.10
B (200, 400, 400)	≈ 0.09	≈ 0.10	≈ 0.09	≈ 0.10
C (400, 500, 400)	≈ 0.09	≈ 0.10	≈ 0.09	≈ 0.10

values of M_{H^\pm} without coming into conflict with the electroweak precision data, and to large values of $\tan\beta$ without coming into conflict with unitarity. However, the large- $\tan\beta$ part is constrained to $M_{H^\pm} \sim 400\text{--}500$ GeV by the electroweak precision data, T in particular. This region roughly corresponds to the decoupling limit. For set C, there are two disconnected, allowed regions.

The little hierarchy.—We show in Fig. 6 the resulting ranges in Λ/\sqrt{D} , as defined by Eq. (5.5). This is seen to reach well beyond 3 TeV, in particular, for set B. Comparing sets of the 2HDM mass parameters it is clear that, in agreement with our expectations, the maximal value of the cutoff Λ/\sqrt{D} grows with the mass scale of the 2HDM model. This illustrates our strategy to ameliorate the little hierarchy problem by lifting the lowest visible Higgs mass. As already mentioned, the allowed regions in this case are very similar to those corresponding to light dark profiles shown in Figs. 1 and 4. This is consistent with the fact that the inert sector influences the experimental constraints only through T which is sensitive to inert scalar-mass splitting. Since the splitting is of the same order (although it is larger for the light dark profiles), therefore, it is not surprising that the allowed regions are similar. Consequently, if we impose a cut on $\Lambda/\sqrt{D} = 2$ TeV we find allowed regions very similar to those found for the lighter dark profiles; see Figs. 3 and 5.

In general, the heavier noninert Higgs states affect the amount of dark matter. However, within the range of parameters explored, their effect can be compensated by a retuning of the soft mass parameter m_η , which for fixed masses yields a calibration of the trilinear inert-noninert Higgs coupling λ_L .

VIII. SUMMARY

We have explored an extension of the inert doublet model [6–8] (IDM), made by replacing the SM Higgs doublet sector by a 2-Higgs-doublet model (2HDM) in order to accommodate CP violation in interactions of neutral Higgs bosons. This model has four inert-sector scalars: two neutral, and a pair of charged ones, as well as three ordinary neutral scalars and an accompanying pair of charged ones. The latter five are those of the familiar 2HDM. Our motivation here was not only to have CP violation in the scalar potential, but also to provide a candidate for dark matter and to ameliorate the little hierarchy problem by lifting Higgs boson masses (thereby increasing the cutoff Λ).

We have estimated the amount of dark matter that is predicted by the model, adopting the code micrOMEGAS [14,15], checking all relevant theoretical and experimental constraints. Solutions were found both for light DM particles, with a mass around 75 GeV, as well as for heavier ones, of the order of a few hundred GeV. In both cases, the splitting between the masses of the charged and the neutral inert scalars must be small in order to reproduce the right

amount of dark matter. In the case of heavier dark matter the splitting is tiny implying nearly vanishing contribution to the T parameter.

As we have noted at the very end of Sec. VII B the regions allowed by the condition $\Lambda/\sqrt{D} > 2$ TeV for lighter and heavier dark matter profiles are similar. This is a consequence of a very small contribution to T from the inert sector (because of the small mass splitting). Since the inert sector influences the experimental constraints only through T , the allowed regions are similar. This observation illustrates an important difference between this model and the original IDM, where the charged inert scalar has to be considerably heavier than the neutral inert scalars in order to provide a contribution to T that can compensate a large negative SM contribution (for a heavy SM Higgs boson). Here the role of the inert sector is mainly restricted to providing a candidate for the dark matter, while T can be made consistent with the data utilizing only the freedom of the 2HDM sector with negligible contribution from the inert sector. That freedom was not available in the original inert model. In our approach the little hierarchy problem is softened by increasing the Higgs boson masses; this is possible mainly through the 2HDM sector alone.

In general, and in agreement with our expectations, the naturality arguments favor heavier 2HDM masses. For instance, if one requires $\Lambda/\sqrt{D} > 2$ TeV, then as seen in the top panel of Fig. 6, only a small region with $\tan\beta \sim 2\text{--}5$ and $M_{H^\pm} \sim 320\text{--}380$ GeV is allowed for $(M_1, M_2, \mu) = (100, 300, 200)$ GeV. In contrast, for heavier 2HDM masses (the middle panel in the same figure) a much larger region remains with $\tan\beta \sim 1\text{--}40$ and $M_{H^\pm} \sim 400\text{--}640$ GeV. On the other hand, for $(M_1, M_2, \mu) = (400, 500, 400)$ GeV (the lower panel) we observe again a large allowed region, which however in this case is split into two disconnected regions corresponding to light ($M_{H^\pm} \sim 300\text{--}450$ GeV) and heavy ($M_{H^\pm} \sim 550\text{--}650$ GeV) charged-Higgs bosons. The splitting is related to partial cancellation between contributions to T from charged and neutral 2HDM scalars. It is worth noting that the pictures which emerge here are similar to the result obtained within the ordinary 2HDM [31] (see also [52]). As we have already mentioned, that similarity follows from the small splitting in the inert doublet-sector masses.

For the light DM scenario discussed in Sec. VII A, the experimental implications (direct detection and production at the LHC) were addressed in [6,8,9]. For the case of heavier DM particles, the prospects are more dim, since the production cross section will be rather small. For a detailed discussion, see [13,53,54].

As for the CP invariance, we observe that in general, CP can be substantially violated in regions allowed by the experimental and theoretical constraints. For instance, it is seen that the electron electric dipole moment can easily exceed the allowed value of $10^{-27}[e\text{ cm}]$ for appropriate choices of the mixing angles. We also note that it is easier

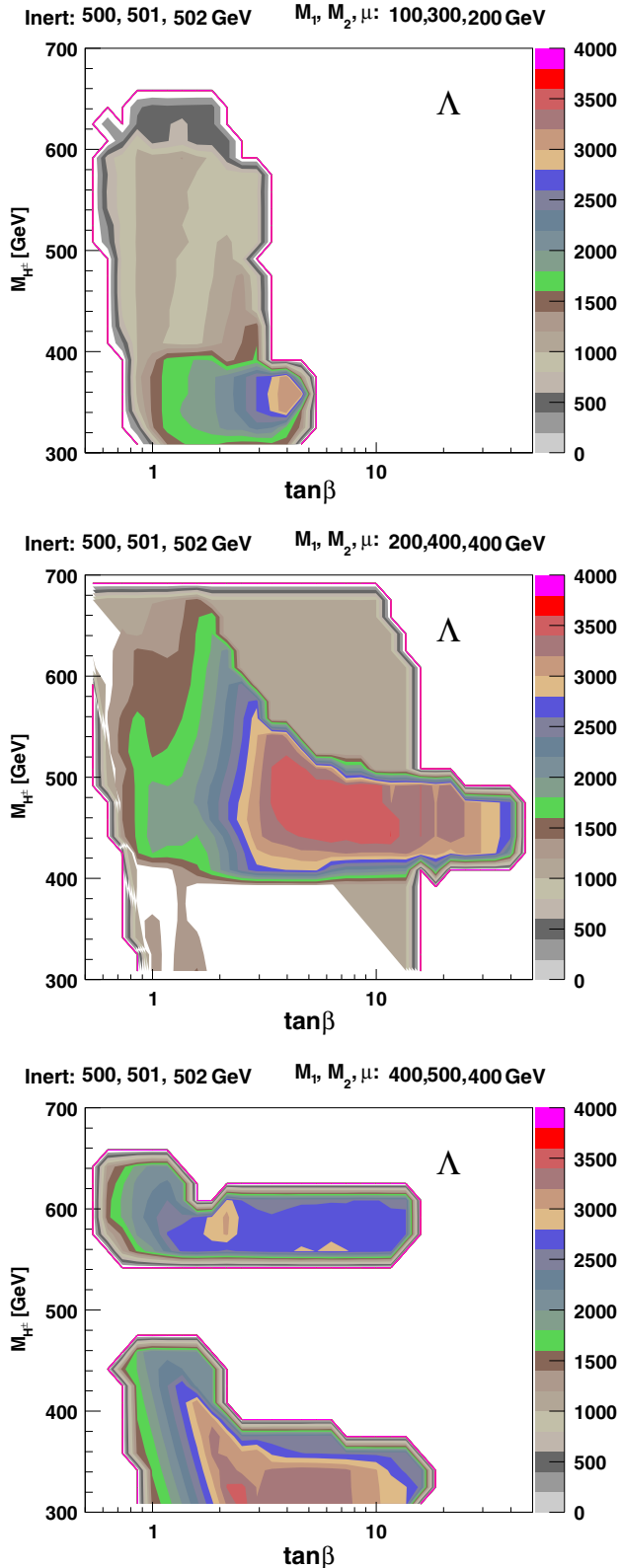


FIG. 6 (color online). Maximum reach in Λ/\sqrt{D} (GeV). Inert-sector masses: (500, 501, 502) GeV; 2HDM-sector masses: $(M_1, M_2, \mu) = (100, 300, 200)$ GeV, $(200, 400, 400)$ GeV, and $(400, 500, 400)$ GeV.

to accommodate CP violation at low values of $\tan\beta$ than at higher values. For high values of $\tan\beta$, the allowed values of $(\alpha_1, \alpha_2, \alpha_3)$ tend to accumulate near the limits where H_2 is odd under CP ($\alpha_2 \simeq 0$, $\alpha_3 \simeq \pm\pi/2$).

It is also worth realizing that the model we discuss here bears some similarity to the Weinberg model [55] of CP violation with natural absence of flavor-changing Yukawa couplings. Both models invoke three doublets, one of which has no Yukawa couplings while the two others couple to fermions such that no flavor-changing Yukawa couplings emerge. However, the important difference is that here (in order to guarantee stability of the dark matter candidate) we impose an extra Z_2 symmetry ($\eta \rightarrow -\eta$) which remains unbroken after spontaneous symmetry breaking since $\langle\eta\rangle = 0$. As a consequence, there is no mixing in the mass matrix between the charged components of $\Phi_{1,2}$ and η , therefore eventually η^\pm is a mass eigenstate with no Yukawa couplings at all. Then CP violation in the charged scalar sector is the same as in a pure 2HDM with Yukawa couplings parametrized by the CKM matrix alone.

It should be noted that restricting our study to the range of inert-model parameters satisfying (2.16), rather than utilizing the full range defined by Eqs. (A16) and (A32), we are clearly not able to find all allowed domains in the parameter space. However, a full investigation is technically much more involved and therefore computationally more challenging. In order to determine all the quartic couplings in the 2HDM sector (V_{12}) one has to specify (M_1, M_2, μ) , $\tan\beta$, M_{H^\pm} and also the angles $(\alpha_1, \alpha_2, \alpha_3)$. To fix the quartic couplings between the 2HDM and the inert sector contained in V_{123} one has to know also the inert mass parameters (M_S, M_A, M_{η^\pm}) and m_η . Then for each point in the parameter space (including angles over which we scan) both Eqs. (A16) and (A32) must be checked. In the presence of the large number of free parameters, that makes the analysis much more complicated and time consuming. Also, within the general strategy outlined here, the calculation of the DM abundance would be much more complicated, since for that purpose all the parameters must be simultaneously known. That is indeed necessary as cross sections for dark matter annihilation depend on the mixing angles $(\alpha_1, \alpha_2, \alpha_3)$, masses of the 2HDM scalars M_1, M_2, M_3 and, of course, also on the inert mass parameters (M_S, M_A, M_{η^\pm}) and m_η . A more complete investigation adopting the general positivity conditions, Eqs. (A16) and (A32), together with a more precise calculation of the dark matter abundance will be attempted, and reported on elsewhere.

ACKNOWLEDGMENTS

We thank NORDITA for hospitality while this work was initiated. It is a pleasure to thank M. Gruenewald for advice on the LEP1 electroweak precision data. We are also grateful to U. Nierste, S. Trine, and S. Westhoff for advice on the

$B \rightarrow D\tau\bar{\nu}_\tau$ analysis, as well as to G. Belanger, A. Pukhov, and M. Tytgat for help with the installation of micrOMEGAS and running the inert doublet model. We thank J. Gunion for his interest at the beginning of this project. The research of P.O. has been supported by the Research Council of Norway. This research of B.G. is supported in part by the Ministry of Science and Higher Education (Poland) as research project No. N202 006334 (2008-11). B.G. also acknowledges support of the European Community within the Marie Curie Research

and Training Networks: HEPTOOLS (MRTN-CT-2006-035505), and UniverseNet (MRTN-CT-2006-035863), and through the Marie Curie Transfer of Knowledge Project MTKD-CT-2005-029466.

APPENDIX A: POSITIVITY OF THE POTENTIAL

In order to ensure vacuum stability, the potential should be positive for large values of the fields Φ_1 , Φ_2 , and η . We study the general potential

$$\begin{aligned} V(\Phi_1, \Phi_2, \eta) = & \frac{\lambda_1}{2}(\Phi_1^\dagger \Phi_1)^2 + \frac{\lambda_2}{2}(\Phi_2^\dagger \Phi_2)^2 + \frac{\lambda_\eta}{2}(\eta^\dagger \eta)^2 + \lambda_3(\Phi_1^\dagger \Phi_1)(\Phi_2^\dagger \Phi_2) + \lambda_4(\Phi_1^\dagger \Phi_2)(\Phi_2^\dagger \Phi_1) + \frac{1}{2}[\lambda_5(\Phi_1^\dagger \Phi_2)^2 + \text{H.c.}] \\ & + \lambda_{1133}(\Phi_1^\dagger \Phi_1)(\eta^\dagger \eta) + \lambda_{2233}(\Phi_2^\dagger \Phi_2)(\eta^\dagger \eta) + \lambda_{1331}(\Phi_1^\dagger \eta)(\eta^\dagger \Phi_1) + \lambda_{2332}(\Phi_2^\dagger \eta)(\eta^\dagger \Phi_2) + \frac{1}{2}[\lambda_{1313}(\Phi_1^\dagger \eta)^2 \\ & + \text{H.c.}] + \frac{1}{2}[\lambda_{2323}(\Phi_2^\dagger \eta)^2 + \text{H.c.}] - \frac{1}{2}\{m_{11}^2 \Phi_1^\dagger \Phi_1 + m_{22}^2 \Phi_2^\dagger \Phi_2 + [m_{12}^2 \Phi_1^\dagger \Phi_2 + \text{H.c.}]\} + m_\eta^2 \eta^\dagger \eta. \end{aligned} \quad (\text{A1})$$

We start by rewriting the Higgs doublets as

$$\Phi_1 = \|\Phi_1\| \hat{\Phi}_1, \quad \Phi_2 = \|\Phi_2\| \hat{\Phi}_2, \quad \eta = \|\eta\| \hat{\eta}, \quad (\text{A2})$$

where $\|\Phi_i\|$ and $\|\eta\|$ are the norms of the spinors, and $\hat{\Phi}_i$ and $\hat{\eta}$ are unit spinors. By $SU(2)$ invariance, only the following combinations of fields may appear:

$$\begin{aligned} \Phi_1^\dagger \Phi_1 &= \|\Phi_1\|^2, & \Phi_2^\dagger \Phi_2 &= \|\Phi_2\|^2, \\ \eta^\dagger \eta &= \|\eta\|^2, & \Phi_2^\dagger \Phi_1 &= \|\Phi_1\| \cdot \|\Phi_2\| (\hat{\Phi}_2^\dagger \cdot \hat{\Phi}_1), \\ \Phi_1^\dagger \Phi_2 &= [\Phi_2^\dagger \Phi_1]^*, & \eta^\dagger \Phi_1 &= \|\Phi_1\| \cdot \|\eta\| (\hat{\eta}^\dagger \cdot \hat{\Phi}_1), \\ \Phi_1^\dagger \eta &= [\eta^\dagger \Phi_1]^*, & \eta^\dagger \Phi_2 &= \|\Phi_2\| \cdot \|\eta\| (\hat{\eta}^\dagger \cdot \hat{\Phi}_2), \\ \Phi_2^\dagger \eta &= [\eta^\dagger \Phi_2]^*. \end{aligned} \quad (\text{A3})$$

We let the norms of Eq. (A2) be parametrized as follows:

$$\begin{aligned} \|\Phi_1\| &= r \cos \gamma \sin \theta, & \|\Phi_2\| &= r \sin \gamma \sin \theta, \\ \|\eta\| &= r \cos \theta. \end{aligned} \quad (\text{A4})$$

The complex product between two different unit spinors will be a complex number with modulus less than or equal to unity, i.e.

$$\begin{aligned} \hat{\Phi}_2^\dagger \cdot \hat{\Phi}_1 &= \rho_1 e^{i\phi_1}, & \hat{\eta}^\dagger \cdot \hat{\Phi}_1 &= \rho_2 e^{i\phi_2}, \\ \hat{\eta}^\dagger \cdot \hat{\Phi}_2 &= \rho_3 e^{i\phi_3}. \end{aligned} \quad (\text{A5})$$

Using this parametrization, we can write

$$\begin{aligned} \Phi_1^\dagger \Phi_1 &= r^2 \cos^2 \gamma \sin^2 \theta, \\ \Phi_2^\dagger \Phi_2 &= r^2 \sin^2 \gamma \sin^2 \theta, \\ \eta^\dagger \eta &= r^2 \cos^2 \theta, \\ \Phi_2^\dagger \Phi_1 &= r^2 \cos \gamma \sin \gamma \sin^2 \theta \rho_1 e^{i\phi_1}, \\ \Phi_1^\dagger \Phi_2 &= r^2 \cos \gamma \sin \gamma \sin^2 \theta \rho_1 e^{-i\phi_1}, \\ \eta^\dagger \Phi_1 &= r^2 \cos \gamma \sin \theta \cos \theta \rho_2 e^{i\phi_2}, \\ \Phi_1^\dagger \eta &= r^2 \cos \gamma \sin \theta \cos \theta \rho_2 e^{-i\phi_2}, \\ \eta^\dagger \Phi_2 &= r^2 \sin \gamma \sin \theta \cos \theta \rho_3 e^{i\phi_3}, \\ \Phi_2^\dagger \eta &= r^2 \sin \gamma \sin \theta \cos \theta \rho_3 e^{-i\phi_3}, \end{aligned} \quad (\text{A6})$$

where $r \geq 0$, $\gamma \in [0, \pi/2]$, $\theta \in [0, \pi/2]$, $\rho_i \in [0, 1]$, and $\phi_i \in [0, 2\pi)$.

The potential can now be written as

$$V = r^4 V_4 + r^2 V_2, \quad (\text{A7})$$

with only the quartic, V_4 , part relevant for positivity,

$$\begin{aligned} V_4 &= \lambda_1 A_1 + \lambda_2 A_2 + \lambda_\eta A_3 + \lambda_3 A_4 + \lambda_4 A_5 + \lambda_{1133} A_6 \\ &+ \lambda_{2233} A_7 + \lambda_{1331} A_8 + \lambda_{2332} A_9 + \text{Re} \lambda_5 A_{10} \\ &+ \text{Im} \lambda_5 A_{11} + \text{Re} \lambda_{1313} A_{12} + \text{Im} \lambda_{1313} A_{13} \\ &+ \text{Re} \lambda_{2323} A_{14} + \text{Im} \lambda_{2323} A_{15}, \end{aligned} \quad (\text{A8})$$

where

$$\begin{aligned}
A_1 &= \frac{1}{2} \cos^4 \gamma \sin^4 \theta, & A_2 &= \frac{1}{2} \sin^4 \gamma \sin^4 \theta, & A_3 &= \frac{1}{2} \cos^4 \theta, & A_4 &= \cos^2 \gamma \sin^2 \gamma \sin^4 \theta, & A_5 &= \rho_1^2 \cos^2 \gamma \sin^2 \gamma \sin^4 \theta, \\
A_6 &= \cos^2 \gamma \sin^2 \theta \cos^2 \theta, & A_7 &= \sin^2 \gamma \sin^2 \theta \cos^2 \theta, & A_8 &= \rho_2^2 \cos^2 \gamma \sin^2 \theta \cos^2 \theta, & A_9 &= \rho_3^2 \sin^2 \gamma \sin^2 \theta \cos^2 \theta, \\
A_{10} &= \rho_1^2 \cos(2\phi_1) \cos^2 \gamma \sin^2 \gamma \sin^4 \theta, & A_{11} &= \rho_1^2 \sin(2\phi_1) \cos^2 \gamma \sin^2 \gamma \sin^4 \theta, & A_{12} &= \rho_2^2 \cos(2\phi_2) \cos^2 \gamma \sin^2 \theta \cos^2 \theta, \\
A_{13} &= \rho_2^2 \sin(2\phi_2) \cos^2 \gamma \sin^2 \theta \cos^2 \theta, & A_{14} &= \rho_3^2 \cos(2\phi_3) \sin^2 \gamma \sin^2 \theta \cos^2 \theta, & A_{15} &= \rho_3^2 \sin(2\phi_3) \sin^2 \gamma \sin^2 \theta \cos^2 \theta.
\end{aligned} \tag{A9}$$

The quartic part of the potential can now be written as

$$\begin{aligned}
V_4 &= \frac{\lambda_1}{2} \cos^4 \gamma \sin^4 \theta + \frac{\lambda_2}{2} \sin^4 \gamma \sin^4 \theta + \frac{\lambda_\eta}{2} \cos^4 \theta + \lambda_3 \cos^2 \gamma \sin^2 \gamma \sin^4 \theta + \lambda_{1133} \cos^2 \gamma \sin^2 \theta \cos^2 \theta \\
&+ \lambda_{2233} \sin^2 \gamma \sin^2 \theta \cos^2 \theta + \rho_1^2 [\lambda_4 + \text{Re} \lambda_5 \cos(2\phi_1) + \text{Im} \lambda_5 \sin(2\phi_1)] \cos^2 \gamma \sin^2 \gamma \sin^4 \theta \\
&+ \rho_2^2 [\lambda_{1331} + \text{Re} \lambda_{1313} \cos(2\phi_2) + \text{Im} \lambda_{1313} \sin(2\phi_2)] \cos^2 \gamma \sin^2 \theta \cos^2 \theta + \rho_3^2 [\lambda_{2332} + \text{Re} \lambda_{2323} \cos(2\phi_3) \\
&+ \text{Im} \lambda_{2323} \sin(2\phi_3)] \sin^2 \gamma \sin^2 \theta \cos^2 \theta.
\end{aligned} \tag{A10}$$

We minimize this expression with respect to ϕ_i to arrive at

$$\begin{aligned}
\bar{V}_4 &= \frac{\lambda_1}{2} \cos^4 \gamma \sin^4 \theta + \frac{\lambda_2}{2} \sin^4 \gamma \sin^4 \theta + \frac{\lambda_\eta}{2} \cos^4 \theta + \lambda_3 \cos^2 \gamma \sin^2 \gamma \sin^4 \theta + \lambda_{1133} \cos^2 \gamma \sin^2 \theta \cos^2 \theta \\
&+ \lambda_{2233} \sin^2 \gamma \sin^2 \theta \cos^2 \theta + \rho_1^2 (\lambda_4 - |\lambda_5|) \cos^2 \gamma \sin^2 \gamma \sin^4 \theta + \rho_2^2 (\lambda_{1331} - |\lambda_{1313}|) \cos^2 \gamma \sin^2 \theta \cos^2 \theta \\
&+ \rho_3^2 (\lambda_{2332} - |\lambda_{2323}|) \sin^2 \gamma \sin^2 \theta \cos^2 \theta.
\end{aligned} \tag{A11}$$

Further, we minimize this expression with respect to ρ_i to arrive at

$$\begin{aligned}
\tilde{V}_4 &= \frac{\lambda_1}{2} \cos^4 \gamma \sin^4 \theta + \frac{\lambda_2}{2} \sin^4 \gamma \sin^4 \theta + \frac{\lambda_\eta}{2} \cos^4 \theta \\
&+ \lambda_x \cos^2 \gamma \sin^2 \gamma \sin^4 \theta + \lambda_y \cos^2 \gamma \sin^2 \theta \cos^2 \theta \\
&+ \lambda_z \sin^2 \gamma \sin^2 \theta \cos^2 \theta,
\end{aligned} \tag{A12}$$

where

$$\lambda_x = \lambda_3 + \min(0, \lambda_4 - |\lambda_5|) \tag{A13}$$

$$\lambda_y = \lambda_{1133} + \min(0, \lambda_{1331} - |\lambda_{1313}|) \tag{A14}$$

$$\lambda_z = \lambda_{2233} + \min(0, \lambda_{2332} - |\lambda_{2323}|). \tag{A15}$$

For the positivity condition to be satisfied, \tilde{V}_4 must be positive for all combinations of $\gamma \in [0, \pi/2]$ and $\theta \in [0, \pi/2]$. This is both a necessary and a sufficient condition.

1. Boundary points

Some points from the parameter space give us some rather simple positivity conditions. We now turn our attention toward these special points.

$\theta = 0$ or $\theta = \pi/2$ or $\gamma = 0$ or $\gamma = \pi/2$.—First we consider the boundary points in the (γ, θ) plane.

$$\tilde{V}_4(\theta = 0) = \frac{\lambda_\eta}{2},$$

$$\tilde{V}_4\left(\theta = \frac{\pi}{2}\right) = \frac{\lambda_1}{2} \cos^4 \gamma + \frac{\lambda_2}{2} \sin^4 \gamma + \lambda_x \cos^2 \gamma \sin^2 \gamma,$$

$$\tilde{V}_4(\gamma = 0) = \frac{\lambda_1}{2} \sin^4 \theta + \frac{\lambda_\eta}{2} \cos^4 \theta + \lambda_y \sin^2 \theta \cos^2 \theta,$$

$$\tilde{V}_4\left(\gamma = \frac{\pi}{2}\right) = \frac{\lambda_2}{2} \sin^4 \theta + \frac{\lambda_\eta}{2} \cos^4 \theta + \lambda_z \sin^2 \theta \cos^2 \theta.$$

The last three of these expressions have the same form as an expression already studied in the 2HDM [20]. Using a result from there, we end up with the following conditions:

$$\begin{aligned}
\lambda_1 &> 0, & \lambda_2 &> 0, & \lambda_\eta &> 0, & \lambda_x &> -\sqrt{\lambda_1 \lambda_2}, \\
\lambda_y &> -\sqrt{\lambda_1 \lambda_\eta}, & \lambda_z &> -\sqrt{\lambda_2 \lambda_\eta}.
\end{aligned} \tag{A16}$$

2. Interior points

What remains is to demand that $\tilde{V}_4 > 0$ also in the interior of the (γ, θ) plane. Thus,

$$\begin{aligned}
\lambda_y \cos^2 \gamma + \lambda_z \sin^2 \gamma &> -\frac{1}{2} \left\{ \frac{\lambda_\eta}{\tan^2 \theta} + (\lambda_1 \cos^4 \gamma + \lambda_2 \sin^4 \gamma \right. \\
&\left. + 2\lambda_x \cos^2 \gamma \sin^2 \gamma) \tan^2 \theta \right\}.
\end{aligned}$$

Maximizing the right-hand side of this inequality with

respect to θ , we find that the maximum occurs at $\tan^2\theta = \sqrt{\lambda_\eta/(\lambda_1\cos^4\gamma + \lambda_2\sin^4\gamma + 2\lambda_x\cos^2\gamma\sin^2\gamma)}$. Substituting this back we arrive at

$$\begin{aligned} & \lambda_y\cos^2\gamma + \lambda_z\sin^2\gamma \\ & > -\sqrt{\lambda_\eta(\lambda_1\cos^4\gamma + \lambda_2\sin^4\gamma + 2\lambda_x\cos^2\gamma\sin^2\gamma)}. \end{aligned} \quad (\text{A17})$$

We need to solve this inequality subject to the constraints given in (A16). Let us distinguish between four different cases:

Case (a) $\lambda_y \geq 0$ and $\lambda_z \geq 0$.—The inequality (A17) is trivially satisfied.

Case (b) $\lambda_y > 0$ and $\lambda_z < 0$.—The left-hand side of (A17) can be both positive and negative. See details in Sec. A 3.

Case (c) $\lambda_y < 0$ and $\lambda_z > 0$.—The left-hand side of (A17) can be both positive and negative. See details in Sec. A 3. Should be similar to case (b) with λ_y and λ_z interchanged.

Case (d) $(\lambda_y \leq 0 \wedge \lambda_z < 0)$ or $(\lambda_y < 0 \wedge \lambda_z \leq 0)$.—We can now square both sides of the inequality and reverse the inequality sign to get

$$\begin{aligned} & \lambda_y^2\cos^4\gamma + 2\lambda_y\lambda_z\cos^2\gamma\sin^2\gamma + \lambda_z^2\sin^4\gamma < \lambda_\eta(\lambda_1\cos^4\gamma \\ & + \lambda_2\sin^4\gamma + 2\lambda_x\cos^2\gamma\sin^2\gamma) \end{aligned}$$

and finally

$$\begin{aligned} & (\lambda_\eta\lambda_1 - \lambda_y^2)\cos^4\gamma + (\lambda_\eta\lambda_2 - \lambda_z^2)\sin^4\gamma + 2(\lambda_\eta\lambda_x \\ & - \lambda_y\lambda_z)\cos^2\gamma\sin^2\gamma > 0 \end{aligned}$$

which is positive definite if

$$\overline{b^2 - 4ac} \geq 0 \wedge [(x_1 > 0 \wedge \lambda_y + \lambda_z x_1 < 0) \vee (x_2 > 0 \wedge \lambda_y + \lambda_z x_2 < 0)], \quad (\text{A24})$$

where the overline (bar) denotes negation. This expression must be true in order for positivity to be satisfied. The possible solutions read:

Case (b) $\lambda_y > 0$ and $\lambda_z < 0$.—In this case $a > 0$, while c can be both positive, zero or negative. We have to distinguish between these cases. The results are

$$\left[c > 0 \wedge \left(a \geq \frac{c\lambda_z^2}{\lambda_y^2} \vee b > -2\sqrt{ac} \right) \right] \vee c \leq 0, \quad (\text{A25})$$

equivalent to

$$\begin{aligned} & [\lambda_\eta\lambda_1 > \lambda_y^2 \wedge (\lambda_2\lambda_y^2 \geq \lambda_1\lambda_z^2 \vee \lambda_\eta\lambda_x - \lambda_y\lambda_z \\ & > -\sqrt{(\lambda_\eta\lambda_1 - \lambda_y^2)(\lambda_\eta\lambda_2 - \lambda_z^2)})] \vee \lambda_\eta\lambda_1 \leq \lambda_y^2. \end{aligned} \quad (\text{A26})$$

Case (c) $\lambda_y < 0$ and $\lambda_z > 0$.—In this case $c > 0$, while a can be both positive, zero or negative. We need to distin-

$$\lambda_\eta\lambda_x - \lambda_y\lambda_z > -\sqrt{(\lambda_\eta\lambda_1 - \lambda_y^2)(\lambda_\eta\lambda_2 - \lambda_z^2)}. \quad (\text{A18})$$

3. A detailed study of positivity in cases (b) and (c)

We consider the inequality (A17)

$$\begin{aligned} & \lambda_y\cos^2\gamma + \lambda_z\sin^2\gamma \\ & > -\sqrt{\lambda_\eta(\lambda_1\cos^4\gamma + \lambda_2\sin^4\gamma + 2\lambda_x\cos^2\gamma\sin^2\gamma)}. \end{aligned} \quad (\text{A19})$$

Let us introduce $x = \tan^2\gamma$ and transform the inequality into

$$\lambda_y + \lambda_z x > -\sqrt{\lambda_\eta(\lambda_1 + \lambda_2 x^2 + 2\lambda_x x)}, \quad (\text{A20})$$

which must be satisfied for $x > 0$. In order to analyze this we will study the solutions of the equation

$$\lambda_y + \lambda_z x = -\sqrt{\lambda_\eta(\lambda_1 + \lambda_2 x^2 + 2\lambda_x x)}. \quad (\text{A21})$$

Possible solutions of this equation are given by

$$x_{1,2} = \frac{-b \pm \sqrt{b^2 - 4ac}}{2a}, \quad (\text{A22})$$

where $a = \lambda_\eta\lambda_2 - \lambda_z^2$, $b = 2(\lambda_\eta\lambda_x - \lambda_y\lambda_z)$ and $c = \lambda_\eta\lambda_1 - \lambda_y^2$. These possible solutions are obtained by squaring (A21). However, in doing this we may introduce false solutions, that is, solutions of

$$\lambda_y + \lambda_z x = +\sqrt{\lambda_\eta(\lambda_1 + \lambda_2 x^2 + 2\lambda_x x)}. \quad (\text{A23})$$

In order for (A20) to be satisfied we must demand that (A21) does not have any positive real-valued solutions when subject to the constraints already obtained in (A16). That is:

gush between these cases. The results are

$$\left[a > 0 \wedge \left(c \geq \frac{a\lambda_y^2}{\lambda_z^2} \vee b > -2\sqrt{ac} \right) \right] \vee a \leq 0, \quad (\text{A27})$$

equivalent to

$$\begin{aligned} & [\lambda_\eta\lambda_2 > \lambda_z^2 \wedge (\lambda_1\lambda_z^2 \geq \lambda_2\lambda_y^2 \vee \lambda_\eta\lambda_x - \lambda_y\lambda_z \\ & > -\sqrt{(\lambda_\eta\lambda_1 - \lambda_y^2)(\lambda_\eta\lambda_2 - \lambda_z^2)})] \vee \lambda_\eta\lambda_2 \leq \lambda_z^2 \end{aligned} \quad (\text{A28})$$

Combining the results from cases (a)–(d) subject to the constraints of (A16) there are remarkable(!) simplifications. We end up with

$$\begin{aligned} & \sqrt{\lambda_1}\lambda_z + \sqrt{\lambda_2}\lambda_y \geq 0 \vee \lambda_\eta\lambda_x - \lambda_y\lambda_z \\ & > -\sqrt{(\lambda_\eta\lambda_1 - \lambda_y^2)(\lambda_\eta\lambda_2 - \lambda_z^2)} \end{aligned} \quad (\text{A29})$$

as an additional constraint to the ones listed in (A16), or expressed in a more symmetric form

$$\begin{aligned} \sqrt{\lambda_\eta}\lambda_x + \sqrt{\lambda_1}\lambda_z + \sqrt{\lambda_2}\lambda_y \geq 0 \vee \lambda_\eta\lambda_x^2 + \lambda_1\lambda_z^2 + \lambda_2\lambda_y^2 \\ - \lambda_\eta\lambda_1\lambda_2 - 2\lambda_x\lambda_y\lambda_z < 0. \end{aligned} \quad (\text{A30})$$

4. The dark democracy

In the so-called dark democracy (2.14), $\lambda_y = \lambda_z$ and (A17) simplifies to

$$\lambda_y > -\sqrt{\lambda_\eta(\lambda_1\cos^4\gamma + \lambda_2\sin^4\gamma + 2\lambda_x\cos^2\gamma\sin^2\gamma)} \quad (\text{A31})$$

which is satisfied whenever

$$\lambda_y \geq 0 \vee (\lambda_\eta\lambda_x - \lambda_y^2 > -\sqrt{(\lambda_\eta\lambda_1 - \lambda_y^2)(\lambda_\eta\lambda_2 - \lambda_y^2)}). \quad (\text{A32})$$

This constraint combined with the inequalities from (A16) forms a necessary and sufficient condition to guarantee positivity of the potential.

APPENDIX B: CP CONSERVATION

In the general case, the mixing of the different weak neutral states is described by the angles $\{\alpha_1, \alpha_2, \alpha_3\}$ present in the rotation matrix R . There are three simple limits of no CP violation, namely, when either H_1 , H_2 , or H_3 is odd under CP . These limits can all be defined in terms of α_2 and α_3 , as illustrated in Fig. 1 of [17]: H_1 is odd when $\alpha_2 = \pm\pi/2$; H_2 is odd when $\alpha_2 = 0$ and $\alpha_3 = \pm\pi/2$; whereas H_3 is odd when $\alpha_2 = \alpha_3 = 0$. Away from these limits, the model in general violates CP . (Exceptions will be discussed below.)

We display in Figs. 7 and 8 how the allowed regions of the α parameter space are distributed for different choices of the mass parameters and different cuts on $\tan\beta$. These

plots are obtained by collecting all points for which solutions (in terms of $\tan\beta$, M_{H^\pm} , α_1 , α_2 , α_3) are found during a particular scan (indicated by the parameters at the top), and binning them in the α_i variables. In these figures, we also indicate (yellow plane and green lines) limits where there is no CP violation. These figures show that in general, it is much easier to accommodate CP violation at low values of $\tan\beta$ than at higher values.

In addition to the CP -conserving limits mentioned above there exist also other regions in the parameter space which imply CP invariance. In the following we will identify those regions in terms of the scalar masses, $\tan\beta$ and α_i . In this process we will make repeated use of the following identities that follow from the orthogonality of R :

$$\begin{aligned} \mathcal{M}_{11}^2 &= R_{11}^2(M_1^2 - M_2^2) + R_{31}^2(M_3^2 - M_2^2) + M_2^2 \\ \mathcal{M}_{22}^2 &= R_{12}^2(M_1^2 - M_2^2) + R_{32}^2(M_3^2 - M_2^2) + M_2^2 \\ \mathcal{M}_{33}^2 &= R_{13}^2(M_1^2 - M_2^2) + R_{33}^2(M_3^2 - M_2^2) + M_2^2 \\ \mathcal{M}_{12}^2 &= R_{11}R_{12}(M_1^2 - M_2^2) + R_{31}R_{32}(M_3^2 - M_2^2) \\ \mathcal{M}_{13}^2 &= R_{11}R_{13}(M_1^2 - M_2^2) + R_{31}R_{33}(M_3^2 - M_2^2) \\ \mathcal{M}_{23}^2 &= R_{12}R_{13}(M_1^2 - M_2^2) + R_{32}R_{33}(M_3^2 - M_2^2). \end{aligned}$$

In addition we order the masses so that $M_1 \leq M_2 \leq M_3$.

1. $\text{Im}\lambda_5 = 0$

Whenever $\text{Im}\lambda_5 = 0$ we know that CP is conserved. To see when this happens, we note that

$$\begin{aligned} -\frac{v^2}{2}s_\beta \text{Im}\lambda_5 &= \mathcal{M}_{13}^2 \\ &= R_{11}R_{13}(M_1^2 - M_2^2) + R_{31}R_{33}(M_3^2 - M_2^2) \\ -\frac{v^2}{2}c_\beta \text{Im}\lambda_5 &= \mathcal{M}_{23}^2 \\ &= R_{12}R_{13}(M_1^2 - M_2^2) + R_{32}R_{33}(M_3^2 - M_2^2). \end{aligned} \quad (\text{B1})$$

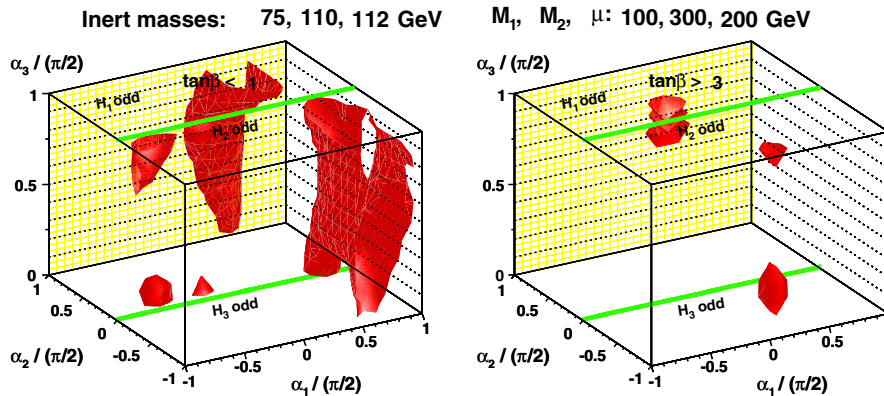


FIG. 7 (color online). Populated regions of α space. Left: $\tan\beta < 1$. Right: $\tan\beta > 3$. Inert-sector masses: (75, 110, 112) GeV. 2HDM-sector masses: $(M_1, M_2, \mu) = (100, 300, 200)$ GeV. Green lines at $\alpha_2 = 0$ (and $\alpha_3 = \pi/2$ or 0) show limits of no CP violation, with either H_2 or H_3 being odd under CP . The limit $\alpha_2 = \pi/2$ (yellow plane) indicates where H_1 is odd. There is a corresponding one at $\alpha_2 = -\pi/2$ (not shown).

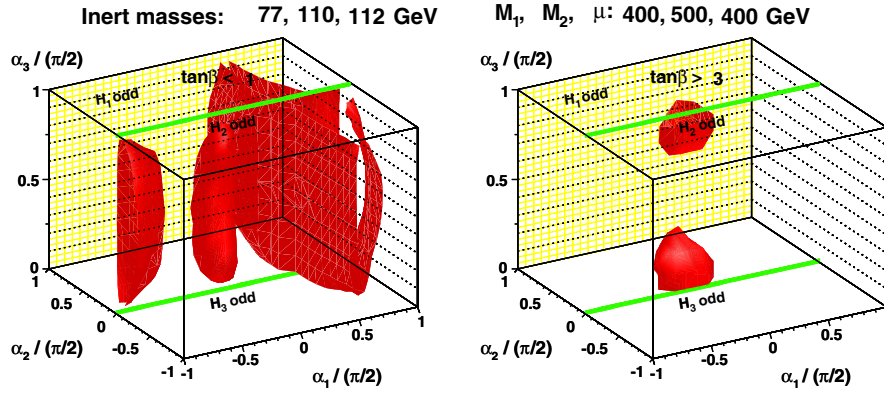


FIG. 8 (color online). Populated regions of α space. Similar to Fig. 7 for inert-sector masses: (77, 110, 112) GeV. 2HDM-sector masses: $(M_1, M_2, \mu) = (400, 500, 400)$ GeV.

Both \mathcal{M}_{13}^2 and \mathcal{M}_{23}^2 must vanish in order to get $\text{Im}\lambda_5 = 0$. (If only one of these quantities vanishes while the other is nonzero, that would correspond to $\beta = 0$ or $\beta = \pi/2$.) That happens in the following cases:

- (1) Full mass degeneracy $M_1 = M_2 = M_3$.
- (2) Lower mass degeneracy $M_1 = M_2 < M_3$, when one of the following conditions is satisfied
 - (a) $\alpha_2 = \pi/2$ or $\alpha_3 = \pi/2$. (This corresponds to $R_{33} = 0$.)
 - (b) $\alpha_2 = 0$ and $\alpha_3 = 0$. (This corresponds to $R_{31} = 0$ and $R_{32} = 0$.)
- (3) Higher mass degeneracy $M_1 < M_2 = M_3$, when one of the following conditions is satisfied:
 - (a) $\alpha_2 = 0$. (This corresponds to $R_{13} = 0$.)
 - (b) $\alpha_2 = \pi/2$. (This corresponds to $R_{11} = 0$ and $R_{12} = 0$.)
- (4) Nondegenerate masses $M_1 < M_2 < M_3$, when one of the following conditions is satisfied:
 - (a) $\alpha_2 = \pi/2$. (This corresponds to $R_{11} = 0$ and $R_{12} = 0$ and $R_{33} = 0$.)
 - (b) $\alpha_2 = 0$ and $\alpha_3 = 0$. (This corresponds to $R_{13} = 0$ and $R_{31} = 0$ and $R_{32} = 0$.)
 - (c) $\alpha_2 = 0$ and $\alpha_3 = \pi/2$. (This corresponds to $R_{13} = 0$ and $R_{33} = 0$.)

2. Partially degenerate masses

We have seen in the previous section that full mass degeneracy implies $\text{Im}\lambda_5 = 0$. However, when $\text{Im}\lambda_5 \neq 0$, partial mass degeneracy is still possible in some cases. We will point out those cases here. We begin by noting that

$$\mathcal{M}_{13}^2 - \tan\beta \mathcal{M}_{23}^2 = 0$$

or, equivalently

$$R_{13}(R_{11} - R_{12} \tan\beta)(M_1^2 - M_2^2) + R_{33}(R_{31} - R_{32} \tan\beta)(M_3^2 - M_2^2) = 0. \quad (\text{B2})$$

- (i) Lower mass degeneracy $M_1 = M_2 < M_3$ is allowed when $R_{31} - R_{32} \tan\beta = 0$. (Excluding $R_{31} = R_{32} =$

0 which would imply $\text{Im}\lambda_5 = 0$ as explained in the previous subsection.)

- (ii) Higher mass degeneracy $M_1 < M_2 = M_3$ is allowed when $R_{11} - R_{12} \tan\beta = 0$. (Excluding $R_{11} = R_{12} = 0$ which would imply $\text{Im}\lambda_5 = 0$ as explained in the previous subsection.)

3. $\lambda_1 = \lambda_2$ and $\tan\beta = 1$

We know that even when $\text{Im}\lambda_5 \neq 0$ we can have cases of CP conservation. One such case is when $\lambda_1 = \lambda_2$ and $\tan\beta = 1$.

$$\begin{aligned} [\lambda_1 - \lambda_2]_{\tan\beta=1} &= \frac{2}{v^2} (\mathcal{M}_{11}^2 - \mathcal{M}_{22}^2) \\ &= \frac{2}{v^2} [(R_{11}^2 - R_{12}^2)(M_1^2 - M_2^2) \\ &\quad + (R_{31}^2 - R_{32}^2)(M_3^2 - M_2^2)]. \end{aligned} \quad (\text{B3})$$

This expression must be zero subject to the constraint (B2) in order to have CP conservation. Thus, when $\text{Im}\lambda_5 \neq 0$ and $\tan\beta = 1$ we have CP conservation in the following cases:

- (1) Lower mass degeneracy $M_1 = M_2 < M_3$ when $R_{31} = R_{32} \neq 0$.
- (2) Higher mass degeneracy $M_1 < M_2 = M_3$ when $R_{11} = R_{12} \neq 0$.
- (3) Nondegenerate masses $M_1 < M_2 < M_3$ in one of the following cases:
 - (a) When $R_{11} = R_{12}$ and $R_{31} = R_{32}$. (Excluding the cases which would imply $\text{Im}\lambda_5 = 0$.) This corresponds to $\alpha_1 = \pi/4$, $\alpha_3 = 0$, and α_2 arbitrary (but not 0 or $\pi/2$).
 - (b) When $R_{11} = R_{12}$ and $R_{33} = 0$ (this implies $R_{31} = -R_{32}$). (Excluding the cases which would imply $\text{Im}\lambda_5 = 0$.) This corresponds to $\alpha_1 = \pi/4$, $\alpha_3 = \pi/2$, and α_2 arbitrary (but not 0 or $\pi/2$).
 - (c) When $R_{31} = R_{32}$ and $R_{13} = 0$ (this implies $R_{11} = -R_{12}$). (Excluding the cases which would imply $\text{Im}\lambda_5 = 0$.) This corresponds to $\alpha_1 = -\pi/4$, $\alpha_2 = 0$, and α_3 arbitrary (but not 0 or $\pi/2$).

4. $\lambda_1 = \lambda_2$ and $(\lambda_1 - \lambda_3 - \lambda_4)^2 = |\lambda_5|^2$

Finally, when $\text{Im}\lambda_5 \neq 0$ we also have CP conservation when $\lambda_1 = \lambda_2$ and $(\lambda_1 - \lambda_3 - \lambda_4)^2 = |\lambda_5|^2$. In order to see what this corresponds to, we start by solving the equation $\lambda_1 = \lambda_2$ for the parameter ν . We find

$$\nu = \frac{s_\beta^2 \mathcal{M}_{11}^2 - c_\beta^2 \mathcal{M}_{22}^2}{v^2 (s_\beta^2 - c_\beta^2)} \quad (\text{B4})$$

when $\lambda_1 = \lambda_2$. Furthermore, we find that

$$\begin{aligned} & (\lambda_1 - \lambda_3 - \lambda_4)^2 - |\lambda_5|^2 \\ &= \left[\frac{1}{c_\beta^2} \left(\frac{\mathcal{M}_{11}^2}{v^2} - \nu s_\beta^2 \right) - \frac{\mathcal{M}_{12}^2}{v^2 s_\beta c_\beta} - \frac{\mathcal{M}_{33}^2}{v^2} \right]^2 \\ & \quad - \left(\frac{\mathcal{M}_{33}^2}{v^2} - \nu \right)^2 - \frac{4}{v^4} [(\mathcal{M}_{13}^2)^2 + (\mathcal{M}_{23}^2)^2]. \end{aligned} \quad (\text{B5})$$

By substituting the expression for ν which is valid when $\lambda_1 = \lambda_2$, we arrive at

$$\begin{aligned} & [(\lambda_1 - \lambda_3 - \lambda_4)^2 - |\lambda_5|^2]_{\lambda_1=\lambda_2} \\ &= \frac{1}{v^4 t_\beta^2 (t_\beta^2 - 1)} \{ t_\beta^2 (1 + t_\beta^2) (\mathcal{M}_{22}^2 - \mathcal{M}_{11}^2) (\mathcal{M}_{22}^2 + \mathcal{M}_{11}^2) \\ & \quad - 2 \mathcal{M}_{33}^2 + 2 t_\beta^3 (1 + t_\beta^2) (\mathcal{M}_{33}^2 - \mathcal{M}_{22}^2) \mathcal{M}_{12}^2 \\ & \quad - 2 t_\beta (1 + t_\beta^2) (\mathcal{M}_{33}^2 - \mathcal{M}_{11}^2) \mathcal{M}_{12}^2 + (t_\beta^2 - 1) (1 + t_\beta^2)^2 \\ & \quad \times (\mathcal{M}_{12}^2)^2 - 4 t_\beta^2 (t_\beta^2 - 1) [(\mathcal{M}_{13}^2)^2 + (\mathcal{M}_{23}^2)^2] \}. \end{aligned}$$

After substituting the mass matrix elements into this expression we get

$$\begin{aligned} & [(\lambda_1 - \lambda_3 - \lambda_4)^2 - |\lambda_5|^2]_{\lambda_1=\lambda_2} = \frac{(M_3^2 - M_2^2)^2 (R_{31} - t_\beta R_{32})}{v^4 t_\beta^2 (1 - t_\beta^2)} \{ (1 + t_\beta^2) (R_{31} + t_\beta R_{32}) (R_{32} - t_\beta R_{31})^2 \\ & \quad + 2 t_\beta R_{33}^2 [(R_{31} (t_\beta^3 - 3 t_\beta) + R_{32} (1 - 3 t_\beta^2))] \} + \frac{(M_1^2 - M_2^2)^2 (R_{11} - t_\beta R_{12})}{v^4 t_\beta^2 (1 - t_\beta^2)} \\ & \quad \times \{ (1 + t_\beta^2) (R_{11} + t_\beta R_{12}) (R_{12} - t_\beta R_{11})^2 + 2 t_\beta R_{13}^2 [(R_{11} (t_\beta^3 - 3 t_\beta) + R_{12} (1 - 3 t_\beta^2))] \} \\ & \quad + \frac{2(M_1^2 - M_2^2)(M_3^2 - M_2^2)}{v^4 t_\beta^2 (1 - t_\beta^2)} \{ (1 + t_\beta^2) (R_{12} - t_\beta R_{11}) (R_{32} - t_\beta R_{31}) (R_{11} R_{31} - t_\beta^2 R_{12} R_{32}) \\ & \quad + t_\beta (1 + t_\beta^2) R_{13}^2 [t_\beta (R_{32}^2 - R_{31}^2) + R_{31} R_{32} (1 - t_\beta^2)] + t_\beta (1 + t_\beta^2) R_{33}^2 [t_\beta (R_{12}^2 - R_{11}^2) \\ & \quad + R_{11} R_{12} (1 - t_\beta^2)] - 4 t_\beta^2 (1 - t_\beta^2) R_{13} R_{33} (R_{11} R_{31} + R_{12} R_{32}) \}. \end{aligned} \quad (\text{B6})$$

This expression must be zero subject to the constraint (B2) in order to have CP conservation. Thus, when $\text{Im}\lambda_5 \neq 0$ and $\tan\beta \neq 1$ we have CP conservation in the following cases:

- (i) Lower mass degeneracy $M_1 = M_2 < M_3$ when $R_{31} = \tan\beta R_{32} \neq 0$ and $\mu^2 = R_{33}^2 M_2^2 + (R_{31}^2 + R_{32}^2) M_3^2$.
- (ii) Higher mass degeneracy $M_1 < M_2 = M_3$ when $R_{11} = \tan\beta R_{12} \neq 0$ and $\mu^2 = R_{13}^2 M_2^2 + (R_{11}^2 + R_{12}^2) M_1^2$.
- (iii) The case of nondegenerate masses $M_1 < M_2 < M_3$ yields several possibilities for CP conservation. To see this we rewrite (B2) as

$$\frac{M_3^2 - M_2^2}{M_2^2 - M_1^2} = \frac{R_{13} (R_{11} - \tan\beta R_{12})}{R_{33} (R_{31} - \tan\beta R_{32})}, \quad (\text{B7})$$

which must be a positive quantity in the case of nondegenerate masses. Solving this equation for $M_3^2 - M_2^2$ and substituting into (B6) we end up with

$$\begin{aligned} & \frac{(M_2^2 - M_1^2)^2 (R_{31} + t_\beta R_{32})}{v^4 R_{33}^2 (R_{31} - t_\beta R_{32})} \frac{(1 + t_\beta^2)}{t_\beta^2 (1 - t_\beta^2)} \\ & \quad \times (R_{11} - t_\beta R_{12}) (R_{11} + t_\beta R_{12}) (R_{21} - t_\beta R_{22}) \\ & \quad \times (R_{21} + t_\beta R_{22}) = 0. \end{aligned} \quad (\text{B8})$$

The solutions of this equation that yield CP conservation are those that also imply positive values of $(M_3^2 - M_2^2)/(M_2^2 - M_1^2)$. They are

- (1) $R_{11} + t_\beta R_{12} = 0$
- (2) $R_{21} + t_\beta R_{22} = 0$
- (3) $R_{31} + t_\beta R_{32} = 0$

provided

$$\frac{R_{13} (R_{11} - \tan\beta R_{12})}{R_{33} (R_{31} - \tan\beta R_{32})} > 0. \quad (\text{B9})$$

5. CP conservation and mass degeneracy

Summarizing the results presented in this Appendix in terms of mass degeneracy we see the following:

- (1) When all three masses are degenerate, CP is conserved because $\text{Im}\lambda_5 = 0$. For this to happen the two input masses must be equal, $M_1 = M_2$. In most

cases [when $R_{33}(R_{31} - R_{32} \tan\beta) \neq 0$] this will lead to M_3 being equal to M_1 and M_2 . If $R_{33}(R_{31} - R_{32} \tan\beta) = 0$ one cannot determine M_3 from the input parameters, but it can be arbitrarily chosen equal to the two other masses.

- (2) When there is only lower mass degeneracy, $M_1 = M_2$ and $R_{33}(R_{31} - R_{32} \tan\beta) = 0$ one cannot determine M_3 from the input parameters, but it can then be arbitrarily chosen to be higher than the two other masses; $M_1 = M_2 < M_3$. CP is then conserved if either:
 - (a) $R_{33} = 0$ or $R_{31} = R_{32} = 0$,
 - (b) $R_{31} = R_{32} \neq 0$ and $\tan\beta = 1$,
 - (c) $R_{31} = R_{32} \tan\beta \neq 0$ and $\tan\beta \neq 1$ and $\mu^2 = R_{33}^2 M_2^2 + (R_{31}^2 + R_{32}^2) M_3^2$.
- (3) When there is only higher mass degeneracy, CP is conserved in some special cases. For this to happen we must first choose $M_1 < M_2$ and $R_{13}(R_{11} - R_{12} \tan\beta) = 0$. Then, if $R_{33}(R_{31} - R_{32} \tan\beta) \neq 0$, $M_2 = M_3$. If $R_{33}(R_{31} - R_{32} \tan\beta) = 0$, one cannot determine M_3 from the input parameters, but it can be arbitrarily chosen to equal M_2 ; $M_1 < M_2 = M_3$. CP is then conserved if either:
 - (a) $R_{13} = 0$ or $R_{11} = R_{12} = 0$,
 - (b) $R_{11} = R_{12} \neq 0$ and $\tan\beta = 1$,
 - (c) $R_{11} = R_{12} \tan\beta \neq 0$ and $\tan\beta \neq 1$ and $\mu^2 = R_{13}^2 M_2^2 + (R_{11}^2 + R_{12}^2) M_3^2$.
- (4) There are also cases of CP conservation in the mass nondegenerate case $M_1 < M_2 < M_3$. For this to happen we must first choose $M_1 < M_2$ and $\alpha_1, \alpha_2, \alpha_3$, and $\tan\beta$ in such a way that $M_3 > M_2$ or in a way such that M_3 cannot be determined from the input parameters. Then M_3 can be arbitrarily chosen to be higher than M_2 . In both cases $M_1 < M_2 < M_3$. CP is then conserved if either:
 - (a) $R_{11} = R_{12} = R_{33} = 0$,
 - (b) $R_{31} = R_{32} = R_{13} = 0$,
 - (c) $R_{13} = R_{33} = 0$,
 - (d) $R_{11} = R_{12}$ and $R_{31} = R_{32}$ (excluding the three cases already mentioned above) and $\tan\beta = 1$,
 - (e) $R_{11} = R_{12} \neq 0$ and $R_{33} = 0$ and $\tan\beta = 1$,
 - (f) $R_{31} = R_{32} \neq 0$ and $R_{13} = 0$ and $\tan\beta = 1$,
 - (g) $R_{11} + R_{12} \tan\beta = 0$ or $R_{21} + R_{22} \tan\beta = 0$ or $R_{31} + R_{32} \tan\beta = 0$ (excluding the three first cases mentioned above) and $\tan\beta \neq 1$, and μ^2 takes on special values.

APPENDIX C: DIFFERENT BASIS

For the purpose of determining the electroweak parameters T and S in Sec. VI, we need to relate the rotation matrix R defined by (2.3) in [20] and the O defined by (59) in [25]. First, we find the U and V (in order to emphasize that the inert doublet is not yet included, we here adopt a subscript 2HDM) of [25] in the basis adopted in [20], where the doublets are denoted by Φ_i [see Eq. (2.6)].

For ϕ_i defined in the basis in which only ϕ_1 has a nonzero VEV (the ‘‘Higgs basis’’) we have

$$\begin{aligned} \phi_1 &= \begin{pmatrix} G^+ \\ (v + H + iG^0)/\sqrt{2} \end{pmatrix} & \phi_2 &= \begin{pmatrix} H^+ \\ (R + iI)/\sqrt{2} \end{pmatrix} \\ \phi_3 &= \begin{pmatrix} \eta^+ \\ (S + iA)/\sqrt{2} \end{pmatrix}. \end{aligned} \quad (C1)$$

The following transformation relates Φ_i and ϕ_j :

$$\begin{pmatrix} \phi_1 \\ \phi_2 \end{pmatrix} = \begin{pmatrix} c_\beta & s_\beta \\ -s_\beta & c_\beta \end{pmatrix} \begin{pmatrix} \Phi_1 \\ \Phi_2 \end{pmatrix}, \quad (C2)$$

with $\phi_3 = \eta$. Since in (C1) the charged-Higgs bosons are mass eigenstates (according to (15) in [25]) we obtain

$$U_{2\text{HDM}} = \begin{pmatrix} c_\beta & s_\beta \\ -s_\beta & c_\beta \end{pmatrix}^T. \quad (C3)$$

The matrix $V_{2\text{HDM}}$ is defined through (see Eq. (60) in [25])

$$\begin{pmatrix} \eta_1 + i\chi_1 \\ \eta_2 + i\chi_2 \end{pmatrix} = V_{2\text{HDM}} \begin{pmatrix} G^0 \\ H_1 \\ H_2 \\ H_3 \end{pmatrix}, \quad (C4)$$

where H_i are mass eigenstates. The rotation matrix R is defined by $H_i = R_{ij} \eta_j$ [see Eq. (2.7)]. Invoking the relation

$$\begin{pmatrix} \chi_1 \\ \chi_2 \end{pmatrix} = \begin{pmatrix} c_\beta & -s_\beta \\ s_\beta & c_\beta \end{pmatrix} \begin{pmatrix} G^0 \\ \eta_3 \end{pmatrix} \quad (C5)$$

and replacing in the left-hand side of (C4) $\eta_{1,2}$ and $\chi_{1,2}$ by the mass eigenstates G^0 and H_j , then $V_{2\text{HDM}}$ is identified as

$$V_{2\text{HDM}} = \begin{pmatrix} ic_\beta R_{11} - is_\beta R_{13} & R_{21} - is_\beta R_{23} & R_{31} - is_\beta R_{33} \\ is_\beta R_{11} + ic_\beta R_{13} & R_{22} + ic_\beta R_{23} & R_{32} + ic_\beta R_{33} \end{pmatrix}. \quad (C6)$$

[1] R. Barbieri and A. Strumia, arXiv:hep-ph/0007265.
 [2] C. F. Kolda and H. Murayama, J. High Energy Phys. 07 (2000) 035; J. A. Casas, J. R. Espinosa, and I. Hidalgo, J. High Energy Phys. 11 (2004) 057.

[3] W. Bernreuther, Lect. Notes Phys. **591**, 237 (2002).
 [4] L. Fromme, S. J. Huber, and M. Seniuch, J. High Energy Phys. 11 (2006) 038.
 [5] B. Grzadkowski and J. Wudka, arXiv:0902.0628.

- [6] R. Barbieri, L. J. Hall, and V. S. Rychkov, *Phys. Rev. D* **74**, 015007 (2006).
- [7] N. G. Deshpande and E. Ma, *Phys. Rev. D* **18**, 2574 (1978).
- [8] Q. H. Cao, E. Ma, and G. Rajasekaran, *Phys. Rev. D* **76**, 095011 (2007).
- [9] L. Lopez Honorez, E. Nezri, J. F. Oliver, and M. H. G. Tytgat, *J. Cosmol. Astropart. Phys.* **02** (2007) 028.
- [10] S. Nie and M. Sher, *Phys. Lett. B* **449**, 89 (1999).
- [11] S. Kanemura, T. Kasai, and Y. Okada, *Phys. Lett. B* **471**, 182 (1999).
- [12] E. Lundstrom, M. Gustafsson, and J. Edsjo, *Phys. Rev. D* **79**, 035013 (2009).
- [13] T. Hambye, F. S. Ling, L. L. Honorez, and J. Rocher, *J. High Energy Phys.* **07** (2009) 090.
- [14] G. Belanger, F. Boudjema, A. Pukhov, and A. Semenov, *Comput. Phys. Commun.* **176**, 367 (2007).
- [15] G. Belanger, F. Boudjema, A. Pukhov, and A. Semenov, *Comput. Phys. Commun.* **180**, 747 (2009).
- [16] W. Khater and P. Osland, *Nucl. Phys.* **B661**, 209 (2003).
- [17] A. W. El Kaffas, P. Osland, and O. M. Ogreid, *Nonlinear Phenom. Complex Syst.* **10**, 347 (2007).
- [18] J. F. Gunion and H. E. Haber, *Phys. Rev. D* **67**, 075019 (2003).
- [19] L. Lavoura and J. P. Silva, *Phys. Rev. D* **50**, 4619 (1994).
- [20] A. W. El Kaffas, W. Khater, O. M. Ogreid, and P. Osland, *Nucl. Phys.* **B775**, 45 (2007).
- [21] S. Kanemura, T. Kubota, and E. Takasugi, *Phys. Lett. B* **313**, 155 (1993).
- [22] A. G. Akeroyd, A. Arhrib, and E. M. Naimi, *Phys. Lett. B* **490**, 119 (2000); A. Arhrib, arXiv:hep-ph/0012353.
- [23] I. F. Ginzburg and I. P. Ivanov, arXiv:hep-ph/0312374; *Phys. Rev. D* **72**, 115010 (2005).
- [24] J. F. Gunion and H. E. Haber, *Phys. Rev. D* **72**, 095002 (2005).
- [25] W. Grimus, L. Lavoura, O. M. Ogreid, and P. Osland, *J. Phys. G* **35**, 075001 (2008).
- [26] W. Grimus, L. Lavoura, O. M. Ogreid, and P. Osland, *Nucl. Phys.* **B801**, 81 (2008).
- [27] C. Amsler *et al.* (Particle Data Group), *Phys. Lett. B* **667**, 1 (2008).
- [28] L. F. Abbott, P. Sikivie, and M. B. Wise, *Phys. Rev. D* **21**, 1393 (1980); G. G. Athanasiu, P. J. Franzini, and F. J. Gilman, *Phys. Rev. D* **32**, 3010 (1985); S. L. Glashow and E. Jenkins, *Phys. Lett. B* **196**, 233 (1987); C. Q. Geng and J. N. Ng, *Phys. Rev. D* **38**, 2857 (1988); **41**, 1715(E) (1990).
- [29] T. Inami and C. S. Lim, *Prog. Theor. Phys.* **65**, 297 (1981); **65**, 1772(E) (1981).
- [30] J. Urban, F. Krauss, U. Jentschura, and G. Soff, *Nucl. Phys.* **B523**, 40 (1998).
- [31] A. W. El Kaffas, P. Osland, and O. M. Ogreid, *Phys. Rev. D* **76**, 095001 (2007).
- [32] K. G. Chetyrkin, M. Misiak, and M. Munz, *Phys. Lett. B* **400**, 206 (1997); **425**, 414(E) (1998); A. J. Buras, A. Kwiatkowski, and N. Pott, *Phys. Lett. B* **414**, 157 (1997); **434**, 459(E) (1998); C. Bobeth, M. Misiak, and J. Urban, *Nucl. Phys.* **B574**, 291 (2000); P. Gambino and M. Misiak, *Nucl. Phys.* **B611**, 338 (2001); A. J. Buras, A. Czarnecki, M. Misiak, and J. Urban, *Nucl. Phys.* **B631**, 219 (2002).
- [33] F. M. Borzumati and C. Greub, *Phys. Rev. D* **58**, 074004 (1998).
- [34] M. Misiak and M. Steinhauser, *Nucl. Phys.* **B683**, 277 (2004); K. Melnikov and A. Mitov, *Phys. Lett. B* **620**, 69 (2005); M. Misiak *et al.*, *Phys. Rev. Lett.* **98**, 022002 (2007); M. Misiak and M. Steinhauser, *Nucl. Phys.* **B764**, 62 (2007); M. Czakon, U. Haisch, and M. Misiak, *J. High Energy Phys.* **03** (2007) 008.
- [35] C. W. Bauer, *Phys. Rev. D* **57**, 5611 (1998); **60**, 099907(E) (1999); M. Neubert, *Eur. Phys. J. C* **40**, 165 (2005).
- [36] P. Krawczyk and S. Pokorski, *Phys. Rev. Lett.* **60**, 182 (1988).
- [37] G. Abbiendi *et al.* (OPAL Collaboration), *Phys. Lett. B* **520**, 1 (2001).
- [38] K. Ikado *et al.*, *Phys. Rev. Lett.* **97**, 251802 (2006); T. E. Browder, *Nucl. Phys. B, Proc. Suppl.* **163**, 117 (2007); B. Aubert (BABAR Collaboration), in *Proceedings of the Thirty-third International Conference on High Energy Physics (ICHEP 06), Moscow, Russia, 2006* (World Scientific, Singapore, 2007).
- [39] W. S. Hou, *Phys. Rev. D* **48**, 2342 (1993); Y. Grossman and Z. Ligeti, *Phys. Lett. B* **332**, 373 (1994); Y. Grossman, H. E. Haber, and Y. Nir, *Phys. Lett. B* **357**, 630 (1995).
- [40] B. Aubert *et al.* (BABAR Collaboration), *Phys. Rev. Lett.* **100**, 021801 (2008).
- [41] U. Nierste, S. Trine, and S. Westhoff, *Phys. Rev. D* **78**, 015006 (2008); (private communication).
- [42] J. Abdallah *et al.* (DELPHI Collaboration), *Eur. Phys. J. C* **38**, 1 (2004).
- [43] A. Denner, R. J. Guth, W. Hollik, and J. H. Kuhn, *Z. Phys. C* **51**, 695 (1991).
- [44] K. Cheung and O. C. W. Kong, *Phys. Rev. D* **68**, 053003 (2003); D. Chang, W. F. Chang, C. H. Chou, and W. Y. Keung, *Phys. Rev. D* **63**, 091301 (2001).
- [45] B. C. Regan, E. D. Commins, C. J. Schmidt, and D. DeMille, *Phys. Rev. Lett.* **88**, 071805 (2002).
- [46] A. Pilaftsis, *Nucl. Phys.* **B644**, 263 (2002).
- [47] D. Bowser-Chao, D. Chang, and W. Y. Keung, *Phys. Rev. Lett.* **79**, 1988 (1997).
- [48] S. M. Barr and A. Zee, *Phys. Rev. Lett.* **65**, 21 (1990); **65**, 2920(E) (1990).
- [49] A. Pilaftsis and C. E. M. Wagner, *Nucl. Phys.* **B553**, 3 (1999).
- [50] C. L. Bennett *et al.* (WMAP Collaboration), *Astrophys. J. Suppl. Ser.* **148**, 1 (2003); D. N. Spergel *et al.* (WMAP Collaboration), *Astrophys. J. Suppl. Ser.* **148**, 175 (2003); D. N. Spergel *et al.* (WMAP Collaboration), *Astrophys. J. Suppl. Ser.* **170**, 377 (2007); E. Komatsu *et al.* (WMAP Collaboration), *Astrophys. J. Suppl. Ser.* **180**, 330 (2009).
- [51] P. Gondolo, J. Edsjo, P. Ullio, L. Bergstrom, M. Schelke, and E. A. Baltz, *J. Cosmol. Astropart. Phys.* **07** (2004) 008.
- [52] S. Kanemura, S. Moretti, Y. Mukai, R. Santos, and K. Yagyu, *Phys. Rev. D* **79**, 055017 (2009).
- [53] S. Andreas, M. H. G. Tytgat, and Q. Swillens, *J. Cosmol. Astropart. Phys.* **04** (2009) 004.
- [54] E. Nezri, M. H. G. Tytgat, and G. Vertongen, *J. Cosmol. Astropart. Phys.* **04** (2009) 014.
- [55] S. Weinberg, *Phys. Rev. Lett.* **37**, 657 (1976).